Summer 2019

Enabling High Energy Density Aluminum Anodes for Alkaline Batteries

Xinyi Zhao

ENABLING HIGH ENERGY DENSITY ALUMINUM ANODES FOR ALKALINE BATTERIES

by

Xinyi Zhao

Bachelor of Engineering
Shandong University, 2016

Submitted in Partial Fulfillment of the Requirements

For the Degree of Master of Science in

Chemical Engineering

College of Engineering and Computing

University of South Carolina

2019

Accepted by:

William E. Mustain, Director of Thesis

Chang Liu, Reader

John Monnier, Reader

Michael Gower, Reader

Cheryl L. Addy, Vice Provost and Dean of the Graduate School

ACKNOWLEDGEMENTS

The life of being a graduate student is coming to an end. Looking back on these two years, I not only learned a lot of knowledge, but also matured a lot. First, I would like to express my special thanks of gratitude to my major advisor Dr. William E. Mustain for all of his help, suggestions, patience and kindness on my research and my whole Masters degree period. I am really thankful that I have learned a lot from this experience and gone through many difficulties with the help of my advisor.

I would like to thank the members of my committee for their expertise and support in assisting my research and Masters defense.

I would thank to Dr. Sujan Shrestha who guided me in doing research with great attention to details – from making and running cells to analyzing data, and he also helped me to overcome numerous obstacles that I faced during my research. I would also like to thank Xiong Peng, Ehsan Faegh, Alessandro Palmieri, Benjamin Ng, Yiwei Zheng, Horie Adabi Firouzjaie, Noor Ul Hassan and Travis Omasta in our research group for their assistance, feedback, cooperation and, of course, friendship. It was great sharing laboratory with them during these two years.

I would like to thank all of the professors who taught me at USC and gave me great help and helping me to expand my fundamental knowledge.

Last but not the least, I would like to thank my family and my friends who have provided me moral and emotional support, for encouraging and supporting me, so that I have the motivation to overcome difficulties and move forward.

ABSTRACT

Zn-MnO_2 primary alkaline batteries stood out immediately among all batteries after it was introduced in the late 1980s and has attracted world-wide attention. These batteries have dominated the portable power market for decades as a highly effective energy storage system with high energy density, long life and low self-discharge, dependable safety and other superiorities.

In order to achieve higher cell-level energy density, Aluminum has long been considered a very attractive anode material for alkaline batteries because of its high theoretical capacity (2980 mAh/g; 2.60 Ah/cm^3) and low price. However, some early efforts to utilize aluminum anodes did not succeed in any commercial battery products. The primary hurdle in the adoption of aluminum anodes in alkaline batteries has been the extremely high Al corrosion rates in concentrated KOH electrolytes. At the same time, zinc is the most common anode for primary alkaline batteries, because it is relatively inert in highly concentrated KOH and is one of the most electropositive metals in the electrochemical series.

Therefore, the underlying goal of this thesis is to investigate various methods and environments to deposit Zn layers on top of Al and to evaluate their efficacy in reducing the corrosion rate. Also, if a thin layer of Zn were achieved, the resulting Zn-coated Al materials would maintain the high energy density offered by Al. Different approaches – including electrodeposition and electroless deposition – have been employed to deposit Zn onto Al substrates (including wires and foils).

Zn was first deposited onto Al wires in a 3-electrode cell. Electrolytic bath additives, including chloride ions (Cl^-, from HCl) and polyethylene glycol (PEG), were introduced into the 1M $ZnSO_4$ solution during electrodeposition. The structure and electrochemical behavior of the resulting Zn-coated Al were characterized. The adhesion and crystallinity of the deposits improved with adding Cl^- ions and PEG, and a lower porosity deposit was achieved. All of the films prepared from a 1%PEG + 1M $ZnSO_4$ + ($\leqslant$ 5 ppm) HCl deposition electrolyte showed a 99% reduction in H_2 gassing compared to bare Al wires, and more than twice the capacity of Zn was achieved – though 2.5 ppm Cl^- did show the highest capacity. It was even shown that this deposition process was repeatable with partial discharges.

After successful demonstration of Zn onto Al wires, the project then focused on moving away from wires and examining the creation of Zn-coated Al particles for use in realistic battery systems. 1M $ZnSO_4$ + 1%PEG + 2.5PPM HCl^+ 0.3M Sodium hypophosphite bath was explored for electroless deposition to form Zn-coated Al. The microparticles that were grown were too large to form a thin and efficient layer and due to their wide inter-particle spacing; hence, the sample had a relatively high H_2 gassing rate. It was concluded that electrodeposition was a far more effective method to produce Zn particles than electroless deposition. However, no approaches resulted in Zn-coated Al active materials with acceptably low degradation rates to be seriously considered for commercial applications.

Therefore, an alternative approach to utilizing a portion of the Al capacity while maintaining a low-corrosion material was conceived – to create Zn-rich Al-Zn alloys. With higher Al content in the alloy, it was confirmed that a higher capacity could be achieved.

This result clearly showed that the Al incorporated into the Zn particles could be electrochemically utilized during discharge.

TABLE OF CONTENTS

LIST OF FIGURES

LIST OF TABLES

CHAPTER 1

BACKGROUND AND INTRODUCTION

1.1 Zn-MnO_2 Primary Alkaline Battery

1.1.1 Alkaline Batteries' overview

In the past decades, rapid economic and technological development has always been coupled with the need for all kinds of energy, which allows humans to work and support their lives. Among different types of energy, electrical energy, which can be stored in batteries in the form of chemical energy and then convert that energy into electricity, is pretty vital in our daily life. Batteries can be divided into two major categories, primary batteries and secondary batteries. A primary battery is a disposable kind of battery, which has been widely used in various fields. There are several types of primary batteries, including the traditional alkaline battery, shown in Figure 1.1, which has been a staple of the portable industry for over a half a century. Alkaline batteries derive their name from the electrolyte used in the cell, typically aqueous potassium hydroxide.[1]

Figure 1.1. Primary alkaline batteries.[2]

The alkaline battery stood out immediately among all batteries since it was invented by Lewis Urry in 1957 because of many useful advantages. Alkaline batteries have high specific and volumetric capacity and are one of the most cost-effective batteries[3]. The cost of an alkaline battery is much lower than other commercialized cells, such as Nickel-Cadmium or Lithium ion. One of the historical negatives for alkaline batteries (produced before 1996) was that they contained some mercury, whose leakage could pollute the environment and harm human health. However, modern alkaline batteries have removed mercury without sacrificing performance or energy density. Therefore, alkaline batteries can generally be discarded with household garbage without any special disposal techniques and do not need to be recycled, which means they are environmentally friendly. They also have a much longer shelf life compared with other batteries such as chloride-type electrolyte batteries. In addition, alkaline batteries can be stored at room temperature for several years and retain over 90 percent of their original capacity.

In the United States of America, alkaline batteries account for about 80% of manufactured batteries. Globally, more than 10 billion individual batteries are produced each year over the various sizes (e.g. AAA, AA, C, D). The long life and relatively low initial purchase price make alkaline batteries ideal for many household items such as clocks, digital cameras, hand held games, electronic scales, lights, radios, remove-controlled toys, etc. Some of these applications are pictured in Figure 1.2.

The Zn-MnO2 primary alkaline batteries were introduced in the late 1980s and then have been attracted world-wide attention and dominated the portable power market for decades as a highly effective energy storage system of high energy density, long life and low self-discharge, dependable safety and other superiorities. Among military equipment,

Zn-MnO_2 primary alkaline batteries have been extensively deployed because of their convenient use, excellent performance and long storage stability. They are especially useful as power sources for communication equipment such as tactical radio, field telephones and terminal equipment. Under field conditions, charging is extremely difficult while there is no mains so all rely on battery power. They can also be used as auxiliary power for on-base radio stations (which must work 24 hours every day, consuming a large amount of power during the communication) to ensure continuous communication.

Figure 1.2. Application of primary alkaline batteries in radio-controlled aircraft model and electric toys.[4]

1.1.2 Zn-MnO_2 Primary Alkaline Batteries' Mechanism

As is shown in Figure 1.3, a Zn-MnO_2 primary alkaline battery traditionally consists of i) a positive electrode cathode that is a compressed paste of electrolytic manganese dioxide, electrolyte and carbon (for conductivity); and ii) a negative electrode anode that is composed of micro-scale Zn particles dispersed in a gel electrolyte containing concentrated potassium hydroxide.[5] The hollow center of the cathode is lined with an ion-conducting

separator in order to prevent contact of the electrode materials and short-circuiting of the cell. During discharge, zinc, MnO_2 and water are consumed. Though OH^- participates in the half-reactions, equal amounts of OH^- are consumed and produced. However, the water loss during operation does mean that the effective pH increases as the discharge proceeds.

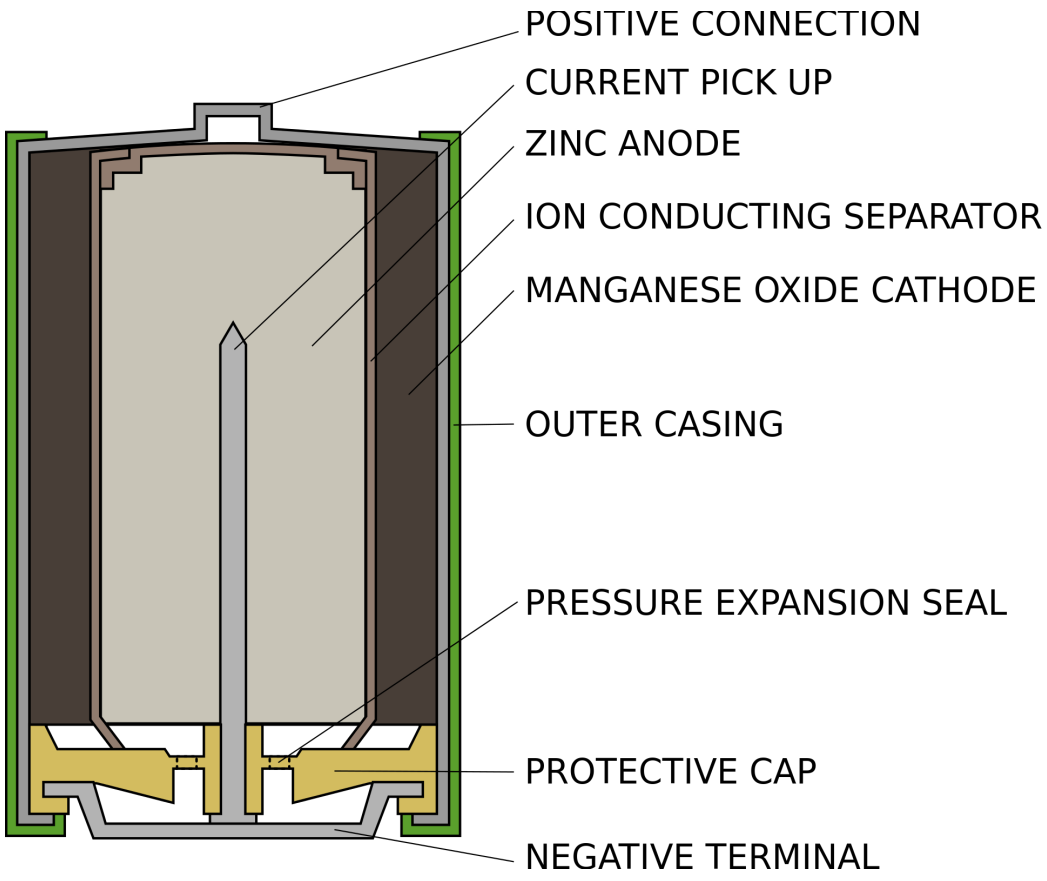

Figure 1.3. Cross-sectional view through a Zn-MnO_2 primary alkaline battery.[6]

An illustration of the operating principles for the Zn-MnO_2 primary alkaline battery is shown in Figure 1.4. The oxidation reactions of Zn (820 mAh/g) and the reduction reactions of MnO_2 (616 mAh/g) take place at anode side and cathode side separated by the

middle separators. The cathode reactions in the positive electrode are as follows[4]: the manganese is reduced from tetravalent to trivalent, undergoing a one electron increment (Equation 1).

$$MnO_2 + H_2O + e^- \rightarrow MnO(OH) + OH^- \quad (1)$$

MnO(OH) has a certain solubility in alkaline solution as is shown in Equation 2:

$$MnO(OH) + H_2O + 3OH^- \rightarrow Mn(OH)_6^{3-} \quad (2)$$

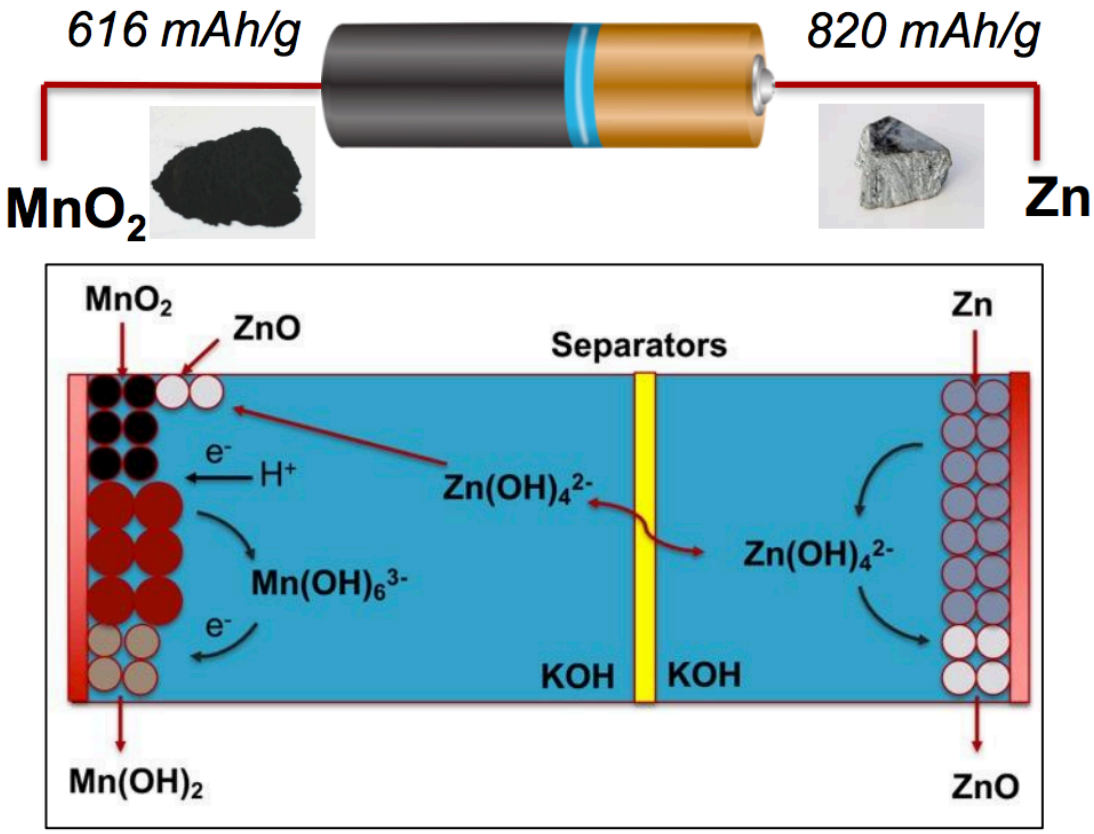

Figure 1.4. Illustration of the working principles of a Zn-MnO_2 primary alkaline battery.[7]

The manganese can theoretically be further reduced from trivalent to divalent (Equation 3), obtaining one electron and increasing the cathode capacity, but in practical batteries this does not occur appreciably because of its low potential – meaning that the cell voltage is too low.

$$e^- + Mn(OH)_6^{3-} \rightarrow Mn(OH)_2 + 4OH^- \quad (3)$$

The anode reactions in the negative electrode are as follows (Equation 4-5): the zinc is increased from zero valence to divalent according to a two electrons oxidation.

$$Zn + 4OH^- \rightarrow Zn(OH)_4^{2-} + 2e^- \quad (4)$$

However, after some time, the produced zincate, $Zn(OH)_4^-$, reaches its solubility limit in the electrolyte and, after the solubility limit is reached, further zincate production is paired with a condensation reaction to produce zinc oxide:

$$Zn(OH)_4^{2-} \rightarrow ZnO + H_2O + 2OH^- \quad (5)$$

The total reaction in the cell is shown in Equation 6:

$$Zn + MnO_2 + H_2O \rightarrow Mn(OH)_2 + ZnO \quad (6)$$

The capacity of Zn-MnO_2 primary alkaline batteries (the amount of charge stored per unit mass – typically reported as mAh/g or Ah/g) is largely limited by the Zn mass in the anode because of its relatively lower theoretical capacity (820 mAh/g_{Zn} or 1.88 Ah/cm^3) than MnO_2. As a result, new anode materials with higher energy density are needed.

1.2 Promise of Aluminum Anodes for Alkaline Batteries

The amount of energy and power that can be delivered from an alkaline battery is a function of many variables, including the cell chemistry, cell balance (cathode/anode ratio), electrolyte loading and concentration, cell void volume, etc. Zinc is the most common

anode for primary alkaline batteries, because it is relatively inert[8] in highly concentrated KOH and is one of the most electropositive metals in the electrochemical series – this means that systems can be designed with relatively low corrosion rates on the shelf and during non-abuse conditions and the anode can have a high capacity. Though capacity can be improved some with additional cell engineering, it is generally accepted that battery manufacturers are approaching the practical energy density and power density limits with the existing Zn-MnO_2 cell chemistry. In order to achieve higher cell-level energy density, new anode material candidates must be either: 1) able to deliver more electrons per reactant than Zn ($2e^-$/Zn), or 2) more electropositive than Zn. Additionally, they must be stable in concentrated aqueous KOH to avoid corrosion and/or self-discharge.

Aluminum has long been considered a "holy grail" anode material for alkaline batteries because of its ability to meet criteria (1) and (2) above as well as its high energy densities and low price[9] and its relatively low atomic mass of 26.98 and its trivalent. This trivalence allows for aluminum to deliver $3e^-$/Al atom. Al is also approximately 280 mV more electropositive than Zn. All of this results in Al having a much higher theoretical gravimetric capacity of 2.98 Ah/g, compared with 0.82 for zinc[10] Its theoretical volumetric capacity is 2.60 Ah/cm^3, which is 1.38 times that of Zn. When translated to the cell level (assuming that the anode and cathode additives all retain typical concentrations for commercial alkaline cells and that the electrolyte, separator and void space volume are the same as a typical commercial cell), aluminum anodes can be expected to increase the cell energy specific energy density by ~19% and the volumetric energy density by 12%, which is shown Table 1.1 below. These metrics would significantly improve the longevity of alkaline batteries.

Table 1.1. Calculated improvements in anode and cell energy density replacing Zn anodes with Al.

Potential Technology Implications	
Increase in Anode Vol Energy Density, %	Increase in Anode Specific Energy Density, %
37.8	44.7
Increase in Cell Energy Density, %	Increase in Specific Energy Density, %
12.0	19.0

However, the performance of batteries using aluminum as anodes is determined by their electrochemical and corrosion properties. Some early efforts that were made to utilize aluminum anodes did not succeed in any commercial battery products. The primary hurdle in the adoption of aluminum anodes in alkaline batteries has been that Al corrosion rates (through Equation 6) are significantly higher than Zn in concentrated KOH electrolytes – roughly 1000 times greater. This means that on-the-shelf corrosion rates, resulting in the production and evolution of H_2 (Equation 6), are unacceptably high[11].

$$2Al(s) + 6H_2O + 2OH^- \rightarrow 2Al(OH)_4^- (aq) + 3H_2 (g) \quad (6)$$

The rate of aluminum corrosion depends on many factors, including $Al(OH)_4^-$ and OH^- concentration in the electrolyte[12]. It is also a hurdle that the primary discharge products from aluminum (i.e. $Al(OH)_3$, Al_2O_3) are insulators, meaning that the cell impedance will increase during discharge. What is needed to transition Al anodes from "holy-grail" status to a practical solution to increasing the energy density of alkaline batteries is a solution that:

1) limits exposure of Al to the electrolyte;

2) maintains electronic conductivity throughout cell discharge.

1.3 **Aluminum Protection by Zn**

There have been several approaches in the literature to reduce the corrosion rate of Al in aqueous alkaline electrolytes. The addition of inhibitors has been used as one of the most common methods to protect aluminum against corrosion in alkaline media[13]. As has been reported, addition of chloride ions or damsissa extract, which could act as effective corrosion inhibitor for the alkaline corrosion of aluminum, to 2M sodium hydroxide solution decreases hydrogen gassing[9]. A compound consisting of the cationic surfactant cetyl trimethyl ammonium bromide (CTAB) and lupine seed extract has also been investigated as an inhibitor of aluminum corrosion in 2 M sodium hydroxide solution and it has been reported to decrease the gas evolution rate on the surface of aluminum[14]. Another family of inhibitors to reduce the rate of alkaline corrosion of Al are three selected polyacrylic acids (PAAs) with different molecular weights; they have been shown to be effective in weakly alkaline solutions (pH 8 and 10)[15]. The use of organic corrosion inhibitors for aluminum in different alkaline (mainly NaOH and KOH) solutions have also been studied such as the mercapto compounds, azole derivatives, organic dyes, and different polymers[16]. At the same time, much attention has been paid to other approaches to reduce the corrosion of Al such as investigating some chemicals as bath additives to the alkaline solutions.

The most effective bath additive to date has been ZnO. The mechanism by which the corrosion rate of Al is decreased in the presence of ZnO is the thermodynamically favored (spontaneous) site exchange reaction of Zn and Al[17]. This results in a Zn coating on the Al

surface, which could increase the overpotential of hydrogen evolution, and if properly structured, the Zn deposition could have a very significant effect on the stability of Al-based active materials when exposed to the battery electrolyte. Such a geometry is illustrated in Figure 1.5. It was also found that the addition of dimethyl amine epoxy propane (designated as DE) could further improve the deposition of zinc layers[18]. From some literature, zinc (and its alloys) have already been used as guard materials for corrosion protection of metals with high corrosion rate such as steel and Aluminum[19]. The gassing rate of Zn-coated Aluminum particles could be significantly reduced compared to the bare aluminum because Zn has acceptably low rates for corrosion and gassing during on-the-shelf and non-abuse discharge conditions.

Unfortunately, the literature working with ZnO still has many unknowns and practical issues. As is reported, the corrosion of aluminum in alkaline solutions (4M KOH) could be effectively inhibited by the bath addition of ZnO, but the poor adhesion of the zinc coatings on the aluminum surface possibly affects the safe use of aluminum anodes in batteries[18]. Other studies suggest that in zincate-containing solutions, an inconsistency has been observed that the open circuit potential of these electrodes was less positive when the zincate coating becomes thicker, which indicates that the formation of Zn coating over the aluminum electrodes are uniform and adherent for the initial moments whereas after a long time this coating shows poor adhesion and exhibits bulging[20]. The most likely reason for this issue would be that spontaneous Zn deposition does not allow the surface potential to be controlled which results that the structure of Zn on the surface also cannot be controlled[21]. Thus, these poor adhesion Zn coatings do not lead to acceptable corrosion rates of Al in alkaline solutions. Besides, there are other practical challenges at such high

KOH and ZnO concentrations, including cell passivation and reduced ion mobility, that make the method of bath additive of ZnO difficult to rely on in practical batteries.

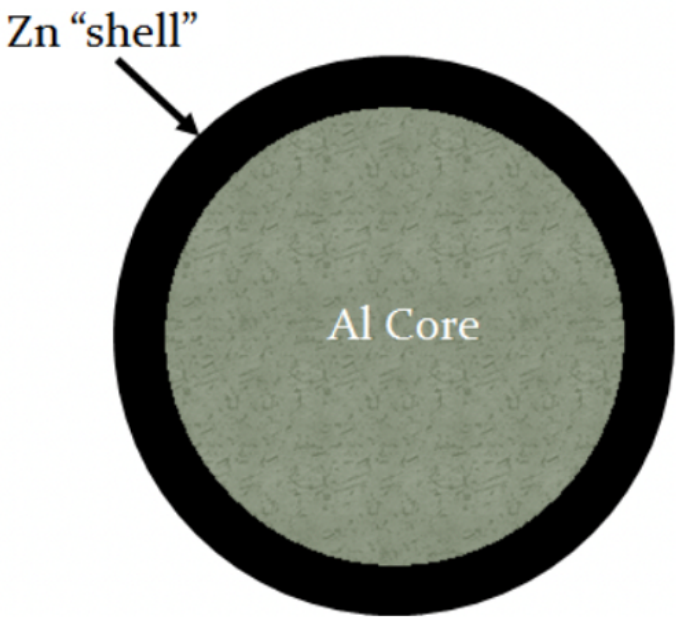

Figure 1.5. Conceptual illustration of Zn-coated Al anodes for primary alkaline batteries.

Therefore, the underlying goal of this thesis is to investigate various methods and environments to deposit Zn layers on top of Al and to evaluate their efficacy in reducing the corrosion rate. Different methods – including electrodeposition and electroless deposition – will be employed to deposit Zn onto Al substrates (including wires and foils). Bath additives will also be introduced into the deposition solution during electrodeposition and electroless deposition, including choride ions (Cl^-, from HCl) and polyethylene glycol (PEG). After deposition, they will be physically and electrochemically characterized. The methods used for these studies are detailed in Chapter 2.

CHAPTER 2

EXPERIMENTS

2.1 Chemicals and Instruments

Table 2.1. List of chemicals used for Zn-coated Al anode preparation.

Chemical Name	**Purity**	**CAS Number**
Zinc Sulfate Heptahydrate (RICCA)	98%	7446-20-0
Zinc Sulfate Heptahydrate	99.995%	7446-20-0
Potassium hydroxide	⩾85%	1310-58-3
Zinc Oxide	⩾99%	1314-13-2
Aluminum powder	99.97%	7429-90-5
Aluminum wire	99.999%	7429-90-5
Nickel wire	99.5%	7440-02-0
Zinc wire	99.99%	7440-66-6
Zinc rod	99.99%	7440-66-6
Nickel foil	99.5%	7440-02-0
Hydrochloric Acid	34-37%	7647-01-0
Polyethylene Glycol 400 (P.E.G)	0.25% max	25322-68-3
Aluminum(III) Chloride	⩾98.0%	7446-70-0

400-Nickel mesh	99.5%	7440-02-0
Sodium Hypophosphite Monohydrate	⩾99%	7681-53-0

Table 2.2. Instrumentation used for cell assembly and characterization.

Type of Instrument	**Manufacturer and Model**
Mass balance	Fisher scientific instrument 01-912-403
Pipette	Thermal scientific 05-403-151
Hotplate	Thermo Scientific 90-691-11
Ultrasonic Cleaning Bath Ultrasonicator	Fisher Scientific instrument 15-337-402
Hg/HgO (/5M KOH) Reference Electrode	CH instruments
$Hg/HgSO_4$ (/Satd K_2SO_4) Reference Electrode	CH instruments
Potentiostat	Autolab PGSTAT302N
Centrifuge	ThermoFisher Scientific Sorvall ST 8
Scanning Electron Microscopy	Zeiss FE - SEMs
Energy Dispersive X-Ray Spectroscopy	Zeiss FE - SEMs
Polypropylene Centrifuge Tubes	Fisher Scientific instrument 12-565-268
Plastic Bottle	Fisher Scientific instrument 03-313-15A
Laboratory Film	Parafilm WI 54956
Injection Syringe	Fisher Scientific instrument NC0526273

Filter Paper	Fisher Scientific 09-795A
Beaker	Fisher Scientific instrument FB10050
Graduated Cylinder	Fisher Scientific instrument 10-462-833
Multi-Colored Timer	Fisher Scientific instrument 02-261-840
Water Purification Systems	Millipore Milli-Q

2.2 Preparation of Solutions

2.2.1 1%PEG-400 + 1M $ZnSO_4$ + 1~5 ppm HCl solution

23g $ZnSO_4$ and 1.03g PEG-400 were added to 80g of 18.2 MΩ.cm deionized (DI) water in a clean plastic tube and mixed well. Then, 8.3uL (34~37%) of HCl was added to 35g of the 1%PEG-400 + 1M $ZnSO_4$ solution to prepare 100 ppm HCl + 1%PEG-400 + 1M $ZnSO_4$ solution. Using the same method, 1%PEG-400 + 1M $ZnSO_4$ + 1-10ppm HCl electrolytes were prepared with different ratios as shown in Table 2.3. The final solutions were sonicated in the Ultrasonicator for 20 minutes to ensure adequate mixing.

Table 2.3. How to prepare electrolytes of 1%PEG-400 + 1M $ZnSO_4$ with varied amount of HCl

1%PEG-400 + 1M $ZnSO_4$ + X ppm HCl	1%PEG-400 + 1M $ZnSO_4$ solution mass (g)	1%PEG-400 + 1M $ZnSO_4$ + Y ppm HCl (mL)
X=10	18	(Y=100) 1.54
X=1	18	(Y=10) 1.54
X=5	10	(Y=10) 7.87

X=2.5	10	(Y=5) 7.87

2.2.2 35% KOH with saturated ZnO electrolyte

For KOH electrolytes containing saturated ZnO, 20g of 18.2 MΩ.cm DI water, 10.77g KOH and excess ZnO powder (1.8g) were mixed in a clean plastic bottle. Then the mixture was heated to its boiling point on a hotplate for 5 minutes and allowed to cool back to room temperature. The mixture was finally centrifuged using the Centrifuge in order to remove the undissolved ZnO solids.

2.2.3 1M $ZnSO_4$ + 0.01~0.05M $AlCl_3$ solution

23g of $ZnSO_4$ and different amounts of $AlCl_3$ (0.193, 0.579, 0.966g) were added to 80g of 18.2 MΩ.cm DI water in clean centrifuge tubes separately. This resulted in 1M $ZnSO_4$ solutions that were also 0.01M, 0.03M, and 0.05M in $AlCl_3$, respectively. The final solutions were sonicated in the Ultrasonicator for 20 minutes to ensure adequate mixing.

2.3 Assembly of Cells and the Gassing Rate Set-up

2.3.1 Three-electrode Cell for Zn Electrodeposition

Eletrodeposition of Zn on Al was conducted in a 3-electrode set-up (shown in Figure 2.1) in which the working electrode was an Al wire (0.81 mm diameter), the counter electrode was spiral Zn wire and the reference electrode was $Hg/HgSO_4$ (saturated K_2SO_4).

The spiral Zn wire was immersed in 50% Nitric Acid for 10 seconds and then sonicated in DI water for 5 min every time before use in order to clean the surface. The reference electrode was rinsed with DI water several times before each use. The Al wire working

electrodes were cleaned by immersing in 35% KOH for 10 seconds to remove its surface oxide film. When introduced to the cell for deposition, the immersion depth was approximately 2 cm. After applying a known current for a prescribed time at room temperature, the Zn films were deposited onto the Al wires. The resulting Zn-coated Al wires were then rinsed with DI water.

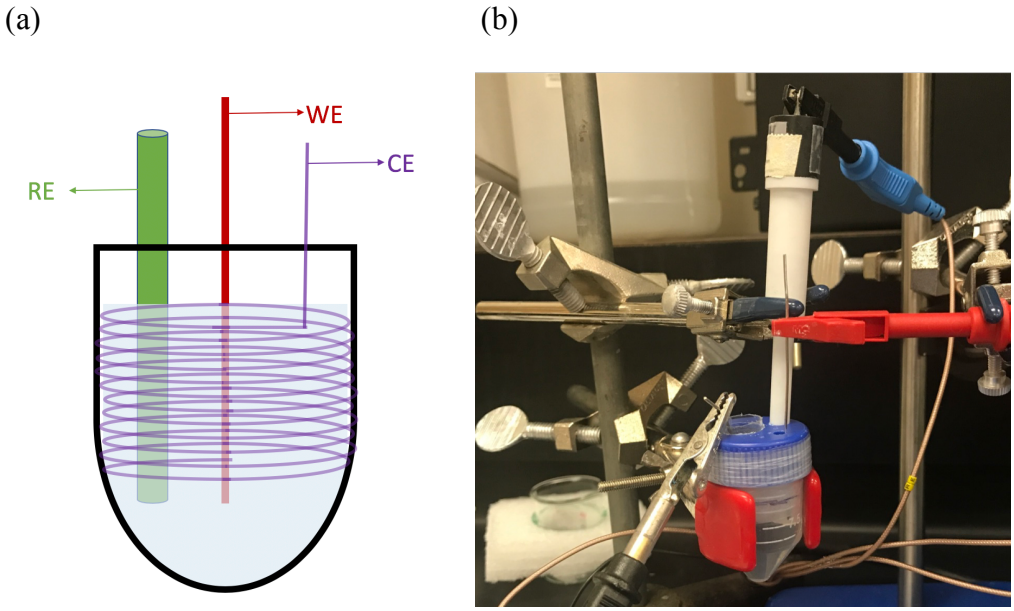

Figure 2.1. (a) Illustration and (b) actual set-up of the 3-electrode cell for electrodeposition.

2.3.2 Three-electrode Cell for Discharge

Discharge experiments of Zn-coated Al were conducted in the same 3-electrode cell that is shown in Figure 2.1(b). In this case, the working electrode was the Zn-coated Al wire, the counter electrode was a spiral Ni wire and the reference electrode was Hg/HgO (5M KOH). The spiral nickel wire was cleaned by immersion in 50% Nitric Acid for 10 s

and then sonicated in DI water for 5 min. Again, the reference electrode was rinsed by DI water several times before using.

2.3.3 Gassing Rate Set-up

Corrosion rates of the Zn-coated Al wires were tested by measuring the volume of hydrogen gas produced through Equation 6 using the custom setup shown in Figure 2.3.2. On the left side, 80uL of DI water and 20uL of Ethanol were mixed in a clean small beaker and then sonicated for 30 minutes to remove the gas in the solution. The small syringe in the upper left part of Figure 2.3.2 was filled with the de-gassed solution. 35% KOH was injected into the larger syringe on the right side of the figure and the Zn-coated Al wire was put into it. Then, a piece of tubing was used to connect the two syringes and the gas displacement was measured. A timer was used to record the gassing time and the amount of gas could be measured from the graduations on the small syringe. The rate of hydrogen evolution was determined by dividing the measured gas volume by the recorded time.

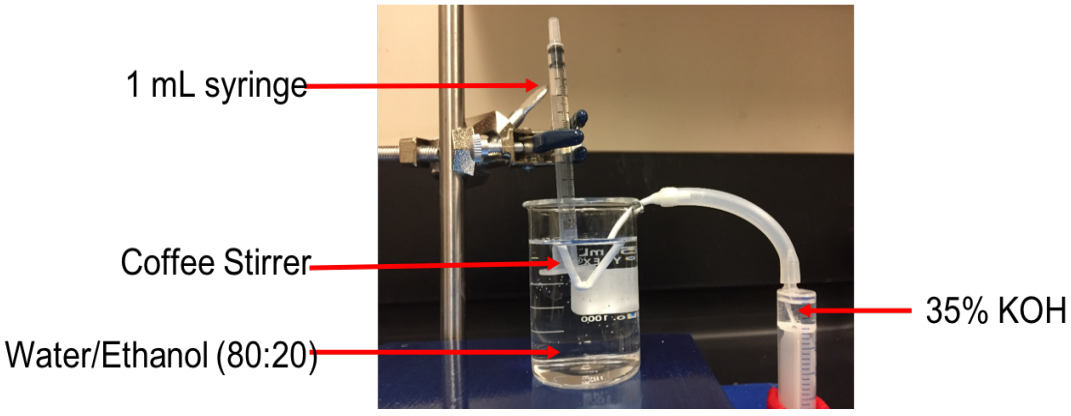

Figure 2.2. Picture of the test set-up for hydrogen gassing.

2.4 Physical and Electrochemical Characterization

2.4.1 Scanning Electron Microscopy

Scanning Electron Microscopy (SEM), was mainly used for visual characterization of material structure,[22] including: grain size, morphology, crystallization and uniformity. During testing, the SEM instrument measures the emission of primary electrons and secondary electrons emitted from the sample surface after they are excited by the beam. SEM is not a surface reflection method, but can image surfaces with outstanding resolution, which would be transformed into two-dimensional images. High magnification and high-resolution images with high depth of field are produced by the SEM. Though transmission electron microscopy can provide even higher magnification images, it only allows for a small portion of the sample to be viewed[23]. Hence, SEM was used to ascertain material morphology and structure in this thesis.

2.4.2 Energy Dispersive X-Ray Spectroscopy

Energy Dispersive X-Ray Spectrometry (EDS) can provide a wide range of elemental detail that is an ideal complement to SEM. When the high energy electron beam in the SEM hits the test sample, electrons are knocked from their orbitals, which causes the electrons from the outer orbitals to fall to those empty positions. In this process, the high energy electrons emit a characteristic x-ray that acts like a finger-print for that particular element. By analyzing this x-ray, detectors can determine the elemental composition. EDS was used to detect the relative elemental abundance of Zn and Al in Zn-coated Al anodes from all of the deposition methods.

2.4.3 Discharge

In this thesis, the discharge performance of the Zn-coated Al anodes were tested with the Autolab potentiostat. This test was operated chronopotentiometrically at a constant current density of 30 mA/cm^2. The discharge current was applied for 3 hours. The use of a constant current makes it very easy to calculate the capacity of a material since it is simply the multiple of the discharge rate, discharge area and time divided by the electrode active material mass – giving the unit: mAh/g. The discharge mass was calculated after each experiment from the sample mass before and after discharge.

2.4.4 Linear Sweep Voltammetry

Linear sweep voltammetry is a voltammetric method where the applied potential between the working electrode and a reference electrode is swept linearly in time and the current at a working electrode is measured at the same time. Linear sweep voltammograms were collected at room temperature between -0.1 and 0.1 V vs. the open circuit potential using the Autolab potentiostat. The scan rate was 0.2 mV/s. The electrolyte was 35% KOH. The reference electrode was Hg/HgO (5M KOH).

CHAPTER 3

RESULTS AND DISCUSSION

One of the fundamental goals of this thesis is to further study how the corrosion rate of aluminum can be reduced via spontaneous coating of the Al particles by Zn (which is thermodynamically favored) in the presence of dissolved ZnO in KOH. Because Zn has acceptably low rates for gassing in commercial application during on-the-shelf and non-abuse discharge conditions, Zn coverage of Al during this time could limit in-cell gassing and self-discharge[14]. Also, if a thin layer of Zn were achieved, the resulting Zn-coated Al materials would maintain the high energy density offered by Al (2980 mAh/g; 2.60 Ah/cm^3). This mechanism for Al protection has been explored fairly extensively in recent years[24], but there has surprisingly been very little truly fundamental information available in the literature regarding ideal coating conditions. The following sections will detail methods to deposit Zn films onto Al substrates, with the deepest focus on Zn electrodeposition onto Al wire electrodes under various experimental conditions.

3.1 Zinc Coating of Al Wires by Electrodeposition

As discussed in Chapter 2, Section 2.3.1, Al wires were initially placed in 1M $ZnSO_4$ solutions and electrodeposition was carried out at multiple current densities in order to determine how the current density affects the structure and efficacy of the resulting Zn

coating. In this first batch of experiments, the deposition time was held constant at 30 minutes. The investigated current densities were 66.7, 76.7, 86,7, and 96.7 mA/cm^2. As shown in Figure 3.1, the thickness, morphology and coverage of the Zn film can be modulated by varying electrodeposition current density. The SEM images revealed that the primary growth mechanism for the Zn film was the seeding of particles that grew into one another to form a film. Higher current density increased the coverage of Zn on the surface, but also increased the average size of an individual Zn particle. Hence, the lowest current density had the best coverage and the highest current density had relatively large inter-particle space, which could allow the electrolyte to access the Al substrate. The roughness and the thickness of the deposits were also affected by the current density, which indicated that the deposits formed at current density of 66.7 mA/cm^2 may have an ideal combination of coverage and the most homogeneous deposits, allowing for the emergence of Zn-protecting films on Al.

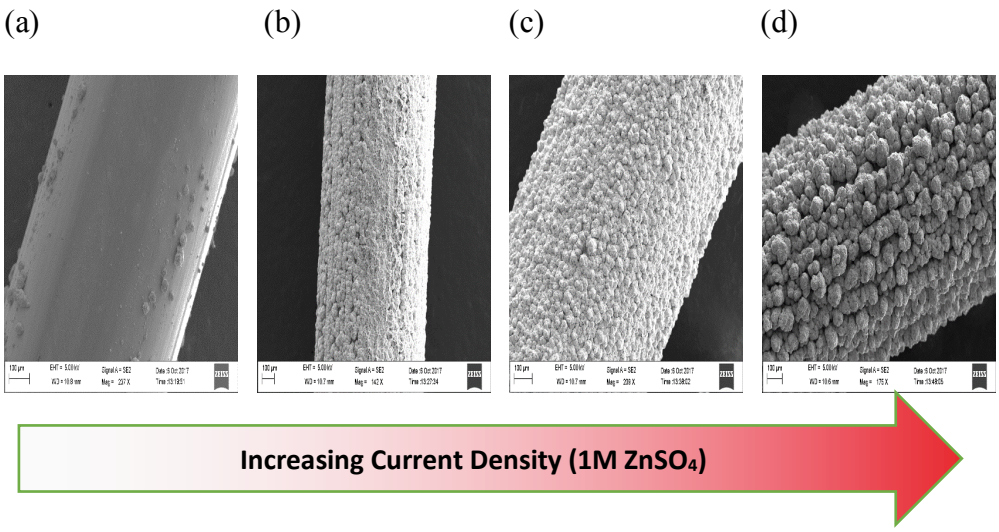

Figure 3.1. SEM images of Zn deposition on Al wires employing increasing current density of (a) 66.7, (b) 76.7, (c) 86,7, and (d) 96.7 mA/cm^2 respectively

A reliable method to directly test for the quality of Al protection is to measure the amount of H_2 gas that is created when the Zn-Al materials are immersed in realistic alkaline electrolytes. As discussed in Chapter 1, H_2 gas is a biproduct of Al corrosion. Therefore, the rate of H_2 production was measured for all of the Zn-deposited Al conditions described above in a 35% KOH electrolyte that was saturated with ZnO. The sample deposited at 66.7 mA/cm^2 in 1M $ZnSO_4$ showed the lowest, but still a relatively high, H_2 gassing rate of 126 uL/min/cm^2. With increased current density, as shown in Figure 3.1.1b-d, the larger Zn particles led to even worse protection as the corrosion of the unprotected Al increased. As a result, these three samples all showed higher H_2 gassing rate of over 130 uL/min/cm^2, suggesting that 66.7 mA/cm^2 may be a the best current density to start from to obtain proper Zn coatings in a 1M $ZnSO_4$ electrodeposition bath. However, the gassing rate with the 66.7 mA/cm^2 current density is higher than desired. For pure Zn wires, identical tests were able to measure essentially zero H_2 gassing for over 20 hours using the same set-up. This would suggest that Al wires with smooth and compact Zn coatings would have similarly low H_2 evolution due to reduced the Al corrosion rate. Our results suggest that despite obvious coating of Al by Zn, there are microstructural defects – even in the best samples – that are allowing electrolyte to access the Al, allowing corrosion to occur.

For this reason, electrolytic bath additives were introduced into the 1M $ZnSO_4$ solution during electrodeposition. Bath additives can be very useful and may be required to improve Zn deposition because of their influence on the growth and structure[25]. Based on the literature, polyethylene glycol (PEG) suppresses the formation of Zn dendrites and Zn deposited with PEG improves rechargeability of secondary Zn-MnO_2 batteries as shown in Figure 3.2. Fractal-like aggregates and dendrite growth were markedly suppressed with

PEG concentrations of 10,000 ppm at both electrode potentials, which indicates with certain PEG concentrations, deposits did not exhibit the classical dendritic morphology[26]. This suggests that PEG may be able to improve the density of the Zn films in this work as well.

To determine whether PEG can affect the electrodeposition of a conformal layer of Zn onto Al, different amounts of PEG-400 from 0, 0.1, 1 to 10 wt% were added to 1M $ZnSO_4$ solutions and investigated as the electrolyte bath. Zn was deposited onto Al wires in these solutions for 30 minutes with an electrodeposition current density of 66.7 mA/cm^2.

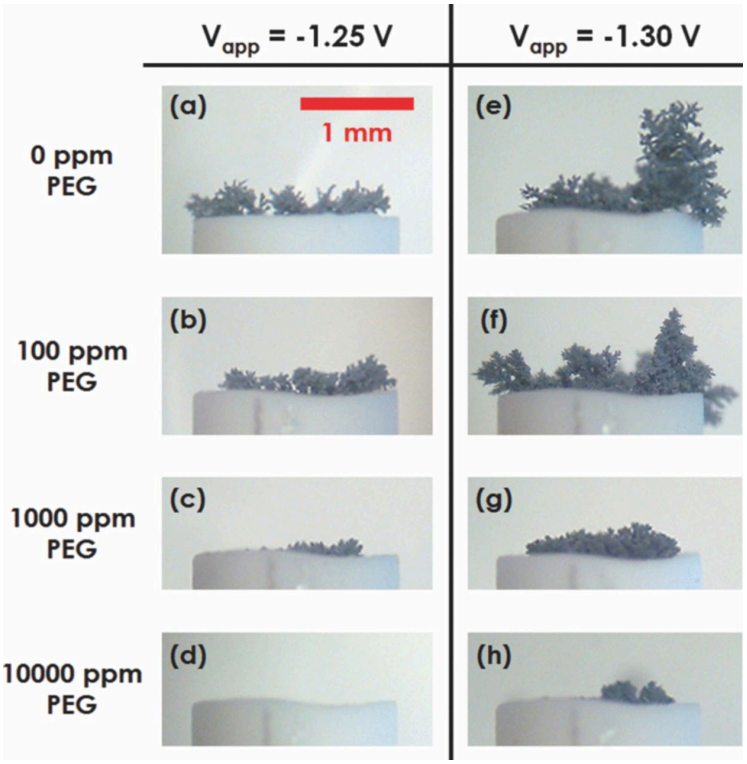

Figure 3.2. Optical microscopy of Zn dendrites from the literature of Suppressing dendrite growth during zinc electrodeposition by PEG-200 additive

The structure and morphology of the resulting Zn-coated Al samples were examined by SEM (Figure 3.3a-c).

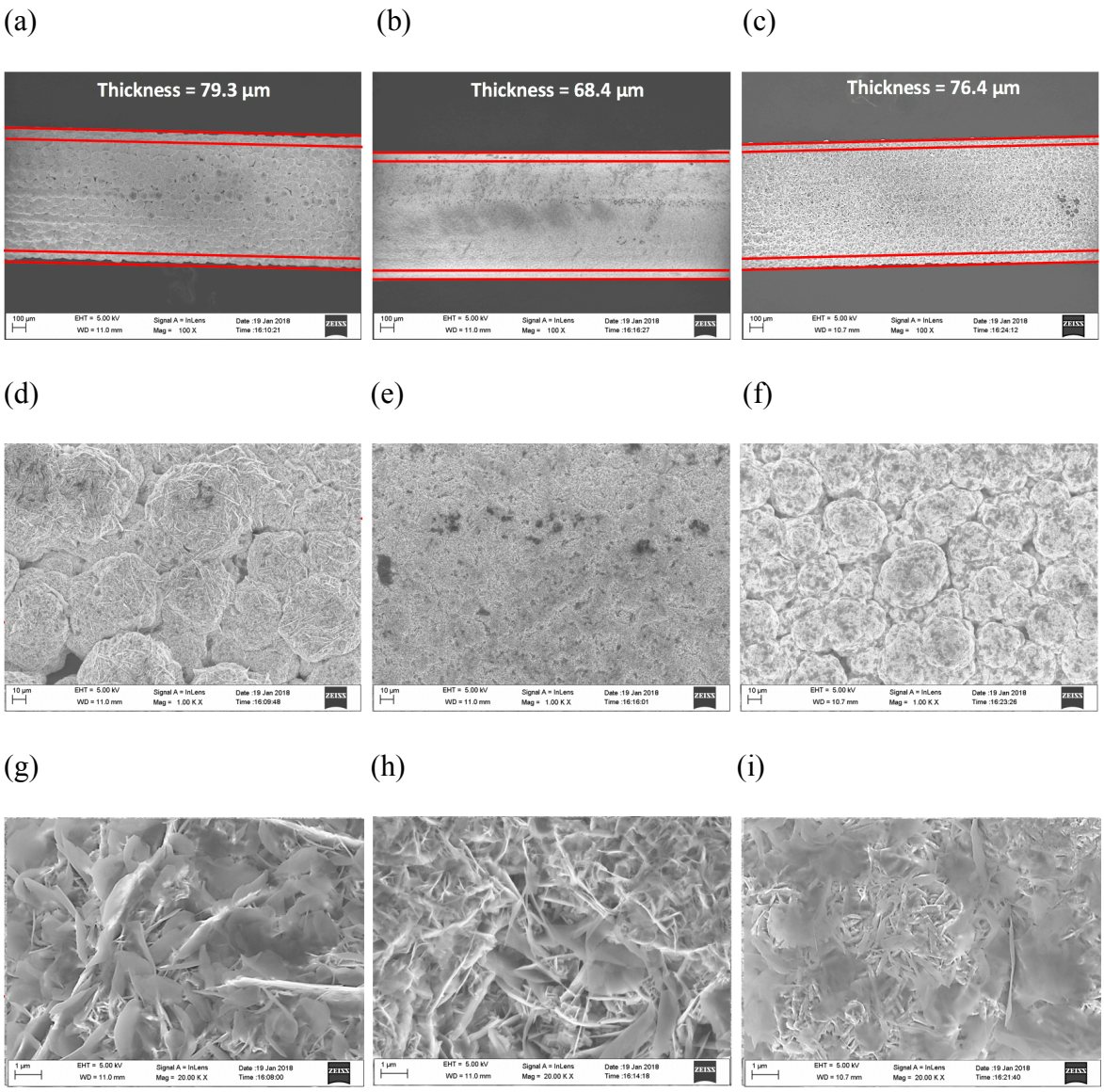

Figure 3.3. SEM images of Zn deposits with (a, d, g) 0.1, (b, e, h) 1, and (c, f, i) 10 % (Wt.) of PEG-400 adding in 1M $ZnSO_4$ electrolyte

Knowing the initial Al wire thickness allowed for the approximate thickness of the Zn surface deposit to be calculated from the images. The samples employing 0.1, 1 and 10 %

PEG concentration had a Zn layer thickness of about 79.3, 68.4 and 76.4 micrometers, respectively, and were all uniformly coated on the Al wires. The thinnest film among these three samples with very similar masses can result in higher effective density than others as well as the least space between the Zn film and Al substrate. From magnified SEM images, Figure 3.3d-f, the coatings present similar spherical Zn microparticles with different size and the second sample employing 1% PEG concentration had the smallest particles while others showed obvious pores in their coatings. The microstructural differences for Zn deposits are further shown at different magnifications in Figure 3.3g-i. Although the morphology of the Zn deposits changes little with PEG concentration, 1% PEG concentration promotes the most uniform growth, which helps to close the inter-particle gaps.

Figure 3.4. shows the Zn deposition potential versus time during the Zn electrodeposition with varied amount of PEG-400 from 0, 0.1, 1 to 10 wt%. As shown illustrated in the plot, at the time below 5 min, as PEG concentration increased from 0.1 to 10 %, the magnitude of the voltage also increased – suggesting that PEG is interacting with the surface of the Al wire. The black line shows that 1% PEG seems to be the optimal condition as verified by SEM characterization. Besides, the deposition started from a relatively high potential; then, after some time, dropped to around -1.3 V (very similar to the Zn-only potential), indicating that the PEG may no longer be affecting the deposition beyond a certain thickness. The open circuit potential (OCP) of Al and Zn in 1M $ZnSO_4$ bath with different PEG concentration was measured before the current was applied. From this plot, relative to 0% PEG, the deposition overpotential increases when adding PEG.

And 1% PEG could improve Zn coating with a little blocking (without affecting Zn deposition too much).

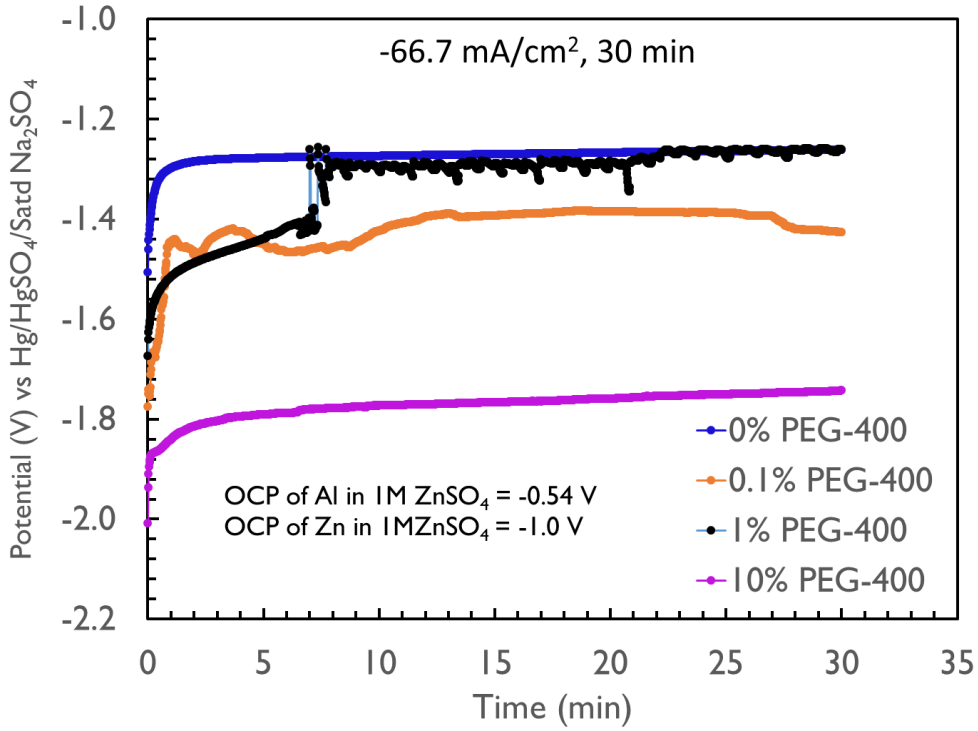

Figure 3.4. Zn deposition potential with 0, 0.1, 1, and 10 % (Wt.) of PEG-400 adding in 1M $ZnSO_4$ electrolyte

The coating of the Zn on the Al wire had a significant effect on the Al stability when exposed to the electrolyte. Table 3.1a shows that the gassing rate of Zn-coated Al wire employing 1% PEG during deposition was significantly reduced compared to bare aluminum and other samples with 0, 0.1 or 10% PEG. In fact, almost no H_2 gas was collected over a 20 hour experiment. For low surface area, or very low H_2 production rate, the gassing rate can be estimated using linear sweep voltammetry. Table 3.1b shows that the fundamental gassing rate for Al coated with Zn is only about 1 order of magnitude less than bare Zn, which means the sample has a very low Al corrosion rate and the Zn coating is effective at protecting the Al from the electrolyte.

Table 3.1. (a) H_2 collection rate for Zn wire and Al coated with Zn samples, (b)OCP and corrosion current for the pure Zn wire and Al coated with Zn samples (N/A means no H_2 gassing was collected for over 20 hours)

(a)

Sample	H_2 collection rate (uL/min/cm^2)
Al wire	113.4
Zn wire	N/A
0%PEG400 + 1M ZnSO4 (66.67 mA/cm^2)	126.0
0.1%PEG400 + 1M ZnSO4 (66.67 mA/cm^2)	20.8
1%PEG400 + 1M ZnSO4 (66.67 mA/cm^2)	N/A
10%PEG400 + 1M ZnSO4 (66.67 mA/cm^2)	115.4

(b)

Sample	OCP (V vs. Hg/HgO/ 5M KOH)	Corrosion Current (A/cm^2)
Zn wire	-1.4	7.12×10-5
1%PEG400 + 1M ZnSO4 (66.67 mA/cm^2)	-1.60	2.68×10-4

The discharge behavior of the Zn-coated Al wires was also investigated. Discharge experiments were conducted at a discharge rate of 30 mA/cm^2 in 35% KOH with saturated ZnO (which could mimic a real battery electrolyte) for 3 hours. The achieved capacity was calculated using Equation 1.

$$Capacity = \frac{discharge\ rate * discharge\ area * time}{mass\ loss} \quad (1)$$

The mass loss was found by weighing the samples before and after the discharge experiment. The discharge area was estimated by the length of the wire exposed to the electrolyte multiplied by the circumference of the Al wire substrate.

The average capacity of the Zn-coated Al anode prepared from a 1% PEG, 1 M $ZnSO_4$ deposition bath was 1817 mAh/g, which is more than twice the theoretical capacity of Zn (820 mAh/g). The high capacity suggests this Zn-coated Al anode could utilize the high energy density offered by Al while at the same time a achieving a robust protecting layer of Zn.

Now that it is known that PEG can help to improve the quality of the Zn deposited onto the Al wire substrate, it is important to understand the other factors that may drive the observed phenomena – such as the presence of impurities. One possible impurity that may play a role in the Zn deposition process is Cl^-, which is present in the $ZnSO_4$ precursor. Cl^- is known to help to adsorb PEG onto the metal surface during Cu electrodeposition through the formation of a PEG-Cu^{2+}-Cl^- complex[27] (Figure 3.5).

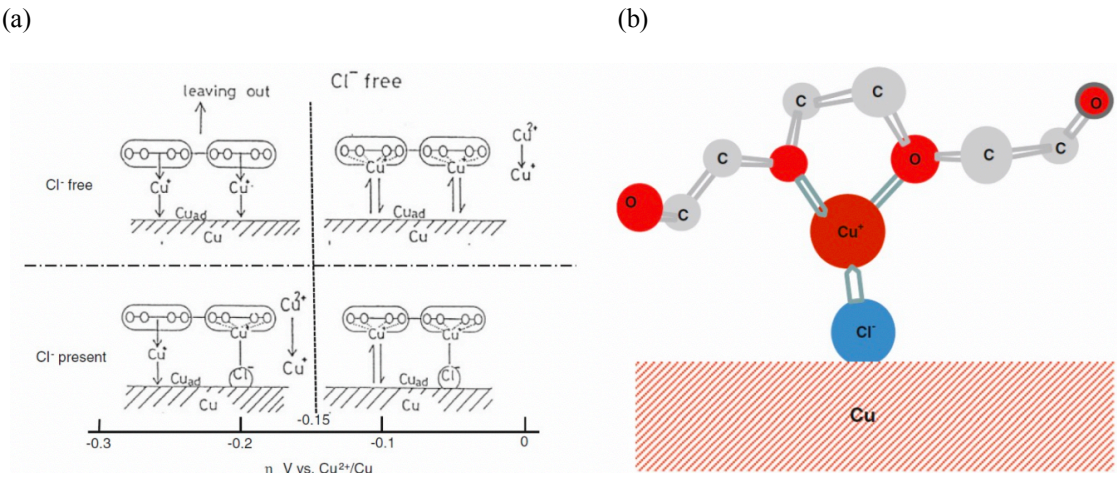

Figure 3.5. Illustration of PEG-Cu^+-Cl^- complex on Cu surface

It is possible that this mechanism may be active here, especially considering that the concentration of the Cl^- impurity is high enough that a 1M $ZnSO_4$ solution may have a Cl^- concentration of 5ppm, which is possibly enough to modify the deposition dynamics. In order to understand if this mechanism was also active in this system, the amount of Cl^- in the electrodeposition bath was systematically varied while holding the PEG and $ZnSO_4$ concentration constant. 1% PEG + 1M $ZnSO_4$ solutions with 1, 2.5 and 5 ppm HCl were prepared. Here, high purity zinc sulfate heptahydrate (99.995%) was used as the Zn source.

The structure and electrochemical behavior of the resulting Zn-coated Al was then characterized. Zoomed out SEM images of Zn deposits (Figure 3.6a-c) with l, 2.5 and 5 ppm Cl^- in the deposition bath show that changing the Cl^- concentration led to very little change in morphology. Additionally, all of the Zn deposits appeared to have tight packing and good adhesion to the substrate. Additional magnification (Figure 3.6d-f) showed no evidence of holes in the films. They all also appeared to have similar flake-like structures. The result was very little hydrogen gassing for all of the films. The average capacities of the Zn-coated Al anodes employing 1, 2.5 and 5 ppm HCl were 1620, 1788.6 and 1565.4 mAh/g, respectively. In other words, all of these films with 1%PEG + 1M $ZnSO_4$ + ($\leq$ 5 ppm) HCl deposition electrolyte showed a significantly reduced reduction in H_2 gassing compared to bare Al wires, and more than twice the capacity of Zn was achieved – though 2.5 ppm Cl^- did show the highest capacity. Therefore, later research added 2.5 ppm HCl to all of the 1%PEG-400 + 1M $ZnSO_4$ solution. It should also be noted that 1620 mAh/g was around 90% of the theoretical capacity for this Zn-coated Al material.

The effect of deposition time was then tested. With a constant current density of 66.7 mA/cm^2, employing 2.5 ppm HCl + 1%PEG-400 + 1M $ZnSO_4$ solution, a range of

deposition times were applied: 10, 15 and 30 min. As the deposition time was decreased, the deposition efficiency improved while the H_2 gassing rate increased because of less Zn coverage. In order to further determine the effect of other variables, including discharge current density and the amount of charge passed (equal to current density multiplied by deposition time), additional tests were conducted.

(a) (b) (c)

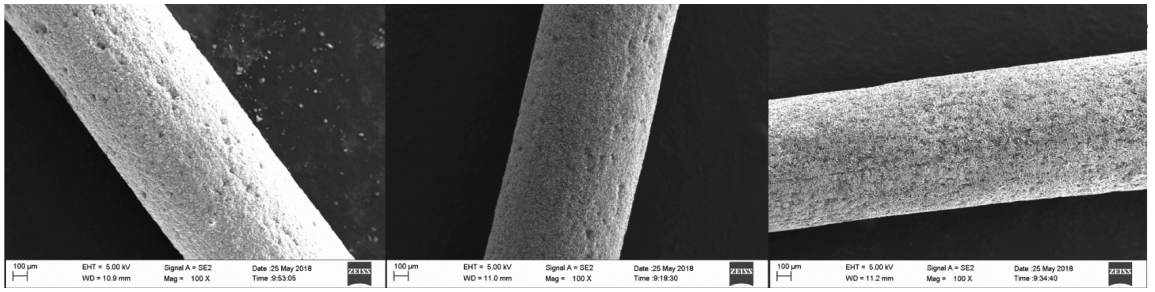

(d) (e) (f)

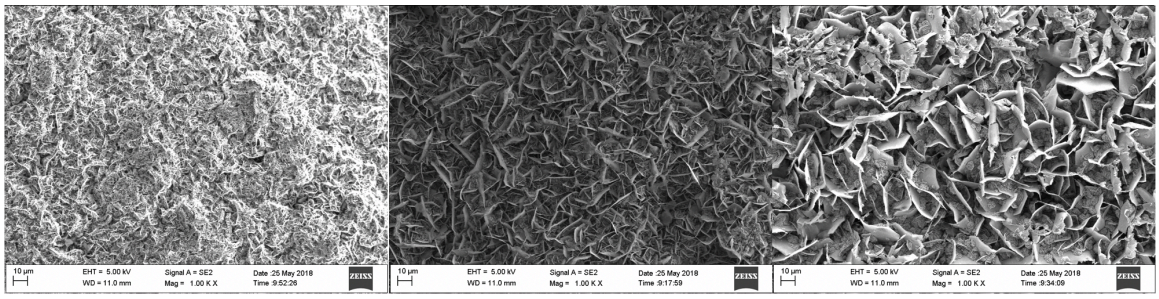

Figure 3.6. Zn deposition on Al wires with different amount of Cl^- of (a, d) 1 ppm (b, e) 2.5 ppm (c, f) 5 ppm.

The results from several experimental trials are shown in Table 3.2. First, identical Zn-coated Al anodes were discharged at a serious of current densities in 35% KOH with saturated ZnO in the electrolyte for a constant discharge time of 3 hours (Table 3.2a). The calculated theoretical capacity for the anodes was 2740 mAh/g, calculated from Equation 2, taking both Al and Zn masses into consideration:

$$Theoretical\ C_{total} = \frac{Deposited\ Zn\ mass * Theoretical\ C_{Zn} + Al\ mass * Theoretical\ C_{Al}}{Total\ mass} \quad (2)$$

The achievable capacity increased with current density because the penetration into the Al is greater with higher current density. At higher current densities, capacities near the theoretical value were achieved. At low current densities, the Zn surface contributed more capacity due to the less penetration to inner Al which led to lower capacities around 1800 mAh/g. At very low current density, 5 mA/cm^2, after discharge the Zn had a very dark, almost black, color. The deposit also had very poor adhesion and it was possible to remove the film simply by gently rinsing the sample. This made it difficult to achieve high capacities. This suggests that a higher discharge current density around 43 mA/cm^2 may lead to a higher capacity, which is close to its theoretical capacity, but a further higher current density may result in discharge loss due to the premature detachment of Zn from the corrosion of Al.

Table 3.2b shows the influence of the current density on the capacity given a constant charge (80 C) in stagnant electrolyte. Faraday's Law was used to calculate the amount of charge. Faraday's law can be summarized by:

$$Q=It \quad (3)$$

where Q is the total electric charge passed through the substance in coulombs, I is the current and t is the discharge time. Capacities are lower in Table 3.2b than Table 3.2a because a higher percentage of the discharge is removing Zn in this case. Also, the highest achieved capacities approach the theoretical limit. However, low and high rate discharges artificially show the best achievable capacity because a low rate with a long discharge time would penetrate the Zn film slowly, which could decrease the corrosion of the exposed Al. And high rate discharge with a short discharge time would utilize the capacity of Al quickly

with less corrosion time. Deposition bath agitation was also tested (Table 3.2c). It was found that introducing convection to the bath increases the achievable capacities but the trend remains the same. Mass transport limitations can lead to local areas of Al exposure with low reaction rate but sustained corrosion.

Table 3.2. (a) Achievable capacity for Zn-coated Al anodes with constant discharge time (b) Influence of the current density on the capacity given a constant charge in stagnant electrolyte (c) Influence of the current density on the capacity given a constant charge in constant stirring electrolyte

(a)

Discharge Current density (mA/cm^2)	Discharge time (s)	Capacity (mAh/g)
50	10800	2084 – premature detachment
43	10800	2408
40	10800	1773.45
30	10800	1788.6
10	10800	1739
5	10800	N/A – adhesion

(b)

Discharge Current Density (mA/cm^2)	Discharge time (h)	Capacity (mAh/g)
80	1.06	1611.4
67	1.25	1602
50	1.68	1445
41	2.1	1572
31	2.8	1504.2
20.2	4.175	1875.2

(c)

Discharge Current Density (mA/cm^2)	Discharge time (h)	Capacity (mAh/g)
80	1.125	1711.5
50	1.8	1620.66
20	4.5	1918.9
15	6	19232.1

To evaluate whether a Zn-coated Al anode could be created from a partially discharged anode, multiple deposition "cycles" were investigated. Here, the Al wire was discharged to different states of charge and Zn coatings with identical thickness were created on the surface after each partial discharge by employing 2.5 ppm HCl + 1%PEG-400 + 1M $ZnSO_4$ solution with the deposition current density of 66.7 mA/cm^2. The experiment is illustrated just above Table 3.3. For all of the depositions, no H_2 gassing was observed over 20 hours – suggesting that it was possible to create a Zn protective coating on not only fresh substrates but used (partially discharged) substrates as well – which speak very highly for the overall approach.

Table 3.3. Simulation and H_2 gassing behavior of Zn-coated Al at various SOC

Diameter (mm)	Deposition time (min)	Current density (mA/cm²)	H2 gassing
0.72	30.3	66.7	N/A over 20 hr
0.66	30.54	66.7	N/A over 20 hr
0.44	32	66.7	N/A over 20 hr

Finally, deposition was done on a single sample that was discharged and re-coated with Zn several times, and the results are shown in Table 3.4. For Al wires, after the same deposition condition and process, no H_2 gassing was detected, which shows that there is not a "memory effect" of the substrate in re-depositing a conformal protective Zn film onto

the Al. This process simulates the Zn-coated Al electrode at different times in a real cell where partial discharges are common and protection of the Al between discharges would be needed.

Table 3.4. Gassing behavior and discharge capacity for Zn-coated Al Electrodes over simulated partial discharges

# of cycles	1st discharge time	1st discharge capacity (mAh/g)	Gassing after 2nd Zn deposition?	2nd discharge time	2nd discharge capacity (mAh/g)	Gassing after 3rd Zn deposition?
2	3h	1557.5	NO			
2	3h	1568.7	NO			
3	3h	1428.7	NO	3h	1647.3	NO
3	3h	1858.3	NO	3h	1607.1	NO

3.2 Electroless Deposition of Zn onto Al

In the previous section, it was shown that it was possible to create a deposition bath (1M $ZnSO_4$ + 1%PEG-400 + 1~5 ppm HCl) for Zn electrodeposition on Al substrates that resulted in a 99% reduction in corrosion and H_2 gassing compared to unprotected Al while achieving more than twice the capacity of Zn-based anodes. It was even shown that this process was repeatable with partial discharges. However, one limitation to the approach above is that alkaline cells typically do not have access to an external power source to force the redeposition of Zn onto Al to protect it during the times where the battery is inactive. Therefore, the most likely source for Zn to deposit on the Al surface is the electrolyte of the alkaline battery itself, which typically contains dissolved ZnO in the form of zincate, $Zn(OH)_4^{2-}$. From thermodynamics, the $Zn(OH)_4^{2-}$ anions should spontaneously deposit onto the Al surface; however, it is not known whether a spontaneous/electroless-type

deposition would be able to result in the same dense, well-protecting layers that were achieved by electrodeposition. Therefore, our attempts were to extend the method to produce Zn-coated Al particles using spontaneous/electroless deposition focused on using zincate-containing systems that accurately mimic the electrolyte in real alkaline batteries. The results of these experiments will be discussed below.

(a)

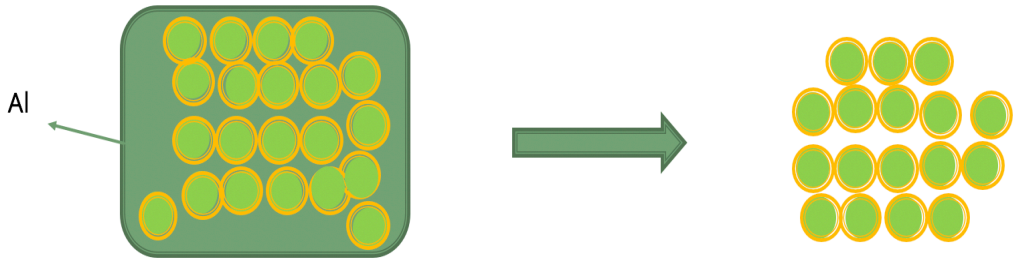

(b)

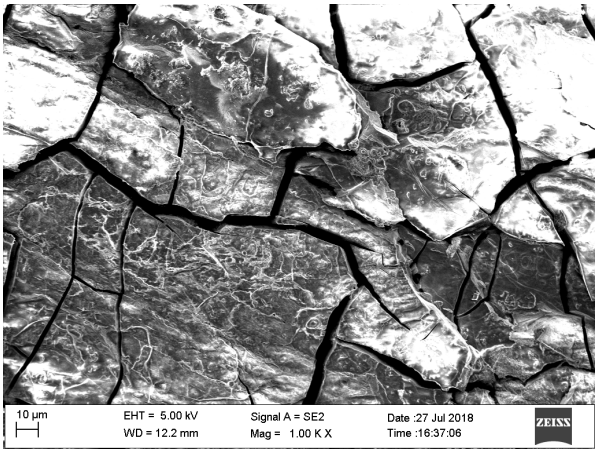

Figure 3.7. (a) Illustration of Al and Zn-coated Al particle deposition
(b) SEM image of Al deposition on Al foil

As illustrated in Figure 3.7a, the first idea for this part of the project was to deposit uniform spherical or oval shaped Al particles onto an Al foil. Then, Zn could be

spontaneously deposited onto the surface of the Al particles. Finally, the particles would be removed, collected and characterized. The desire to create particles was borne from the real application, where particulate anode materials are implemented. However, accomplishing the desired structure was difficult to achieve. As shown in Figure 3.7b, after Al preferred to deposit as a grainy, cracked layer on the foil, not as particles – at least when Al was deposited from aqueous 1M $AlCl_3$ at a current density of 66.7 mA/cm^2.

Due to the difficulty in obtaining Al particles, this approach was abandoned and the next approach was to use existing commercial Al powder and ZnO dissolved into KOH electrolyte. It has already been shown in the literature[28] that Zn can be spontaneously deposited onto an Al surface from ZnO/KOH solutions. However, the coverage and efficacy of the resulting zinc in protecting the Al has been less characterized. 35% KOH with saturated ZnO was used as the electroless bath for the deposition of Zn onto the commercial Al particles. The primary limitation of this approach was that the morphology of the Zn deposit was very porous, as shown in Figure 3.8a-b. The deposit was also very poorly adhered to the substrate and was very easy to remove, which is not ideal. Another item to note about this approach was that the Zn deposits had a very different structure than those created by electrodeposition in 1M $ZnSO_4$ shown earlier in Figure 3.1. This suggests that the surface potential and rate are much different in the case of electrodeposition and electroless deposition. Therefore, it was a logical curiosity whether the same approach used previously to improve the morphology earlier in this chapter, namely adding PEG, would also help here.

Therefore, the next set of experiments used the "optimized" bath that was used for electrodeposition: 1M $ZnSO_4$ + 1%PEG + 2.5PPM HCl – just no current was applied. Here,

Al wires were submerged in the solution for 30 minutes at room temperature. Again, though Zn was able to be formed on the surface, it was found that the Zn film was very poorly adhered to the surface and the coverage was not good (Figure 3.8c).

(a) (b)

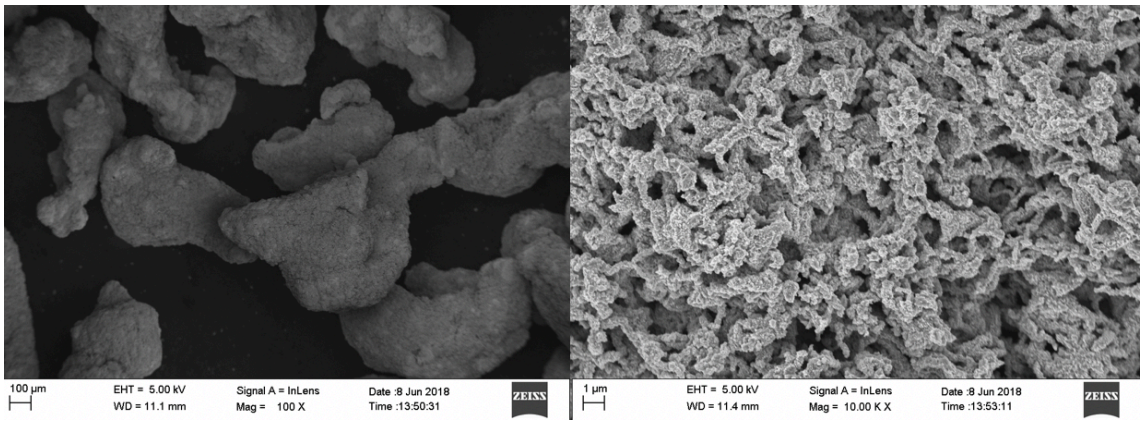

(c)

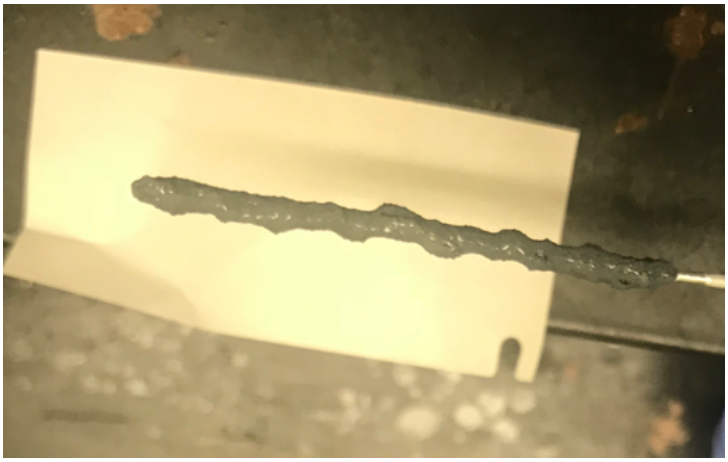

Figure 3.8. (a, b) SEM images of Zn-coated Al particles employing 35% KOH with saturated ZnO (c) Zn-coated Al wire under electroless coating employing "optimized" bath

Literature concerning electroless deposition points to the fact that film adhesion depends on the deposition rate.[29] It was clear here that the electroless deposition rate was

very low, which allowed Al to corrode during deposition, which led to poor attachment. This was also true at longer deposition times, Figure 3.9b-c, though some improvement in the amount of Zn on the surface was observed.

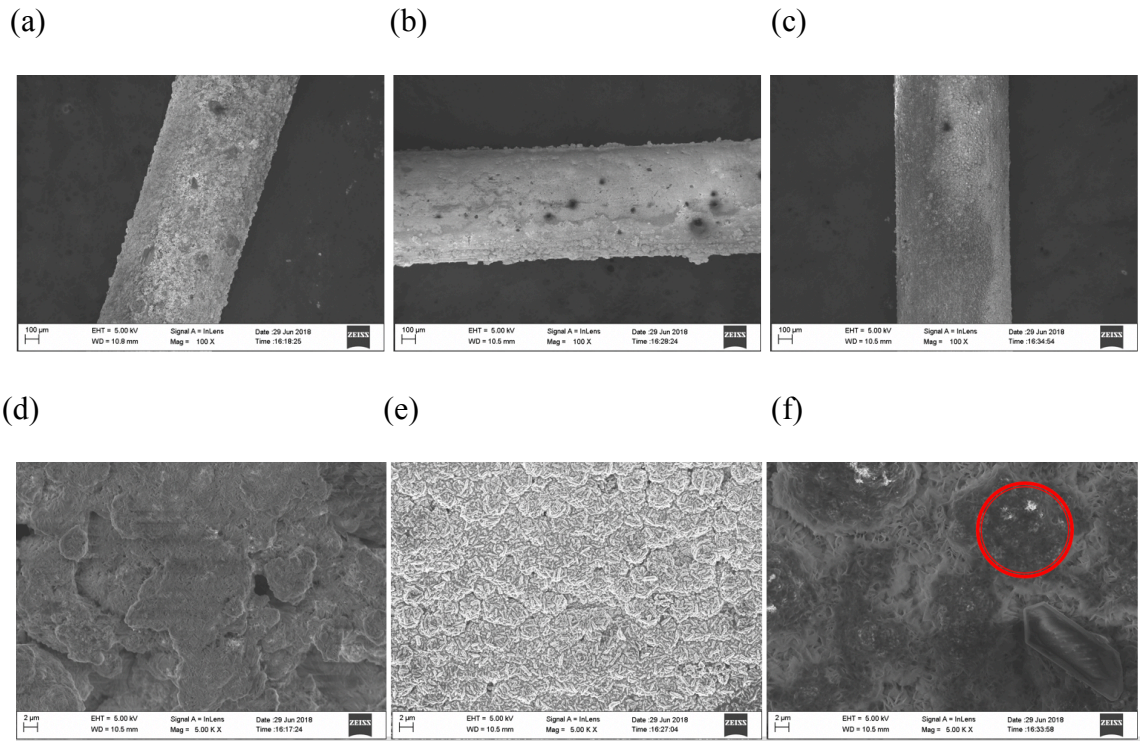

Figure 3.9. SEM images of Al wires after exposure to 1M ZnSO4 + 1%PEG + 2.5PPM HCl baths for (a, d) 30, (b, e) 60 and (c, f) 90 min.

Digging slightly deeper into the SEM images in Figure 3.9, panels a-c, there were obvious holes in the film that were caused by bubbles as a result of hydrogen gassing. Magnified SEM images, panels d-f, show that shorter deposition time led to some dendritic growth initially that, over time, grew bigger as rods and then as flakes. But, as the red circle in Figure 3.9f shows, there were still too many holes in the film at long deposition times, which resulted in a very sparse and porous Zn layer on the Al surface.

One method that was tried to increase the electroless deposition rate, and hence the density and quality of the film, was to introduce other bath additives and possible reducing agents. One such reducing agent was sodium hypophosphite, which has been used in the past for the deposition of Ni-Zn-P materials[30]. A new bath, 1M $ZnSO_4$ + 1%PEG + 2.5PPM HCl + 0.3M Sodium hypophosphite, was then used to deposit Zn onto the Al wire substrate. Additionally, agitation was introduced (stirring the solution at 300 RPM) and the deposition time was increased to 60 minutes. The pH was adjusted to 14 by adding 5M potassium hydroxide according to the following reactions:

$$2KOH + ZnSO_4 \rightarrow K_2SO_4 + Zn(OH)_2\,(s) \quad (\text{less KOH}) \tag{4}$$

$$Zn(OH)_2 + 2KOH \rightarrow K_2ZnO_2 + 2H_2O \quad (\text{excess KOH}) \tag{5}$$

SEM images of Al wires after exposure to the 1M $ZnSO_4$ + 1%PEG + 2.5PPM HCl+ 0.3M Sodium hypophosphite bath are shown in Figure 3.10. Though the microparticles that were grown were too large to form a thin and efficient layer, the coating was compact and made up of loosely-clustered flakes[25]. Due to the inter-particle spacing, the sample had a relatively high H_2 gassing rate, ca. 140 uL/min/cm^2, which is much higher than that of Zn-coated Al anodes employing "optimized" bath eletrodeposition. Other concentrations were tested that are not summarized here because, in the end, a reasonable set of conditions that would allow for the electroless deposition of a conformal Zn coating onto an Al substrate was not discovered, so the concept was abandoned. However, that does not mean that it is not possible to form Zn-Al particles, and a method to do so through electrodeposition – leveraging the successes in Section 3.1 – was attempted, though with a slight twist from the original concept.

(a) (b)

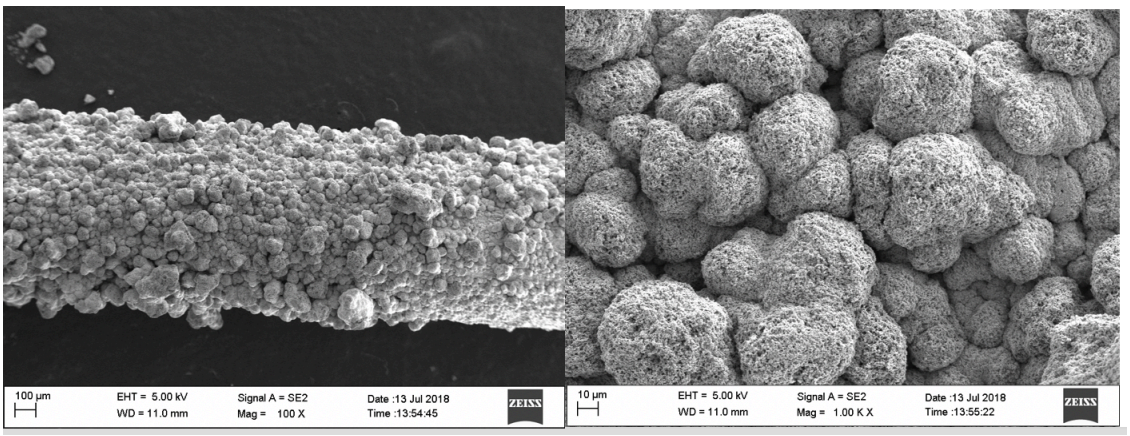

Figure 3.10. SEM images of Al wires after exposure to a new bath (1M ZnSO4 + 1%PEG + 2.5PPM HCl+ 0.3M Sodium hypophosphite) for 60 min.

3.3 Electrochemical Formation of Al-Zn alloy Particles on Ni Mesh Substrates

As shown in the sections above, electrodeposition was a far more effective method to produce Zn particles than electroless deposition. However, it was also shown that the Zn coverage on Al was not perfectly dense, which still allowed Al to be corroded when exposed to the electrolyte. Therefore, an alternative approach to utilizing (at least) some of the Al capacity while maintaining a low-corrosion material is to create Zn-rich Al-Zn alloys. The main reason to include Al is that Al has a much higher specific and volumetric energy density than Zn, which can increase the cell energy density. Though Al has been tried many times as a pure replacement for Zn, it has not yet been successfully implemented because its high corrosion rate (as shown above!) and the low electronic conductivity of passivating Al oxides[9]. However, integrating Al into Zn may provide a capacity boost with a synergistic reduction of the corrosion rate.

(a) (b)

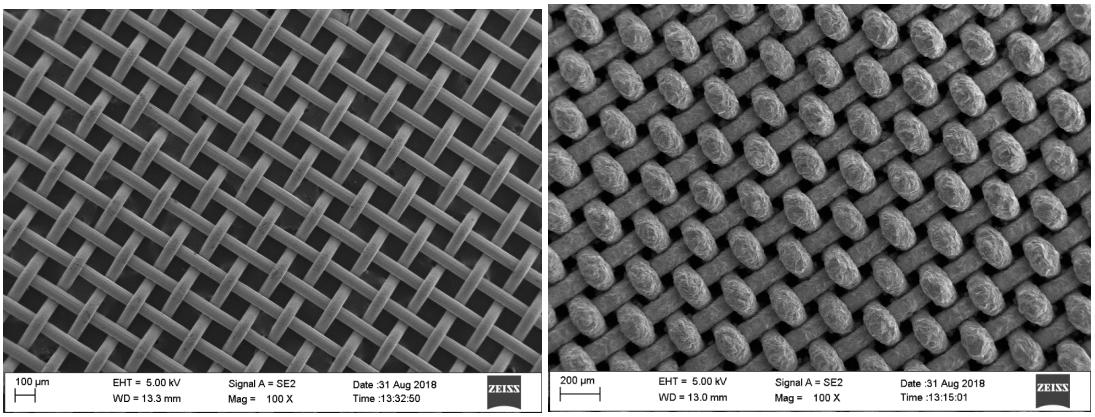

(c) (d)

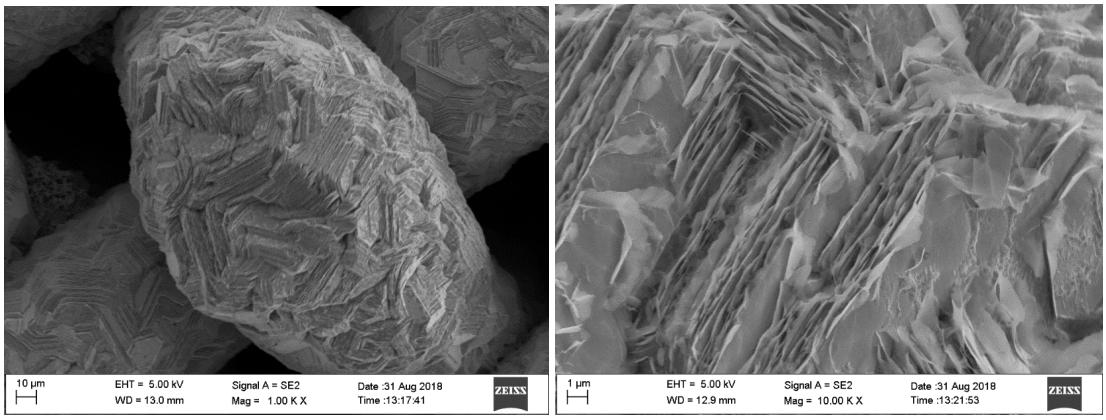

Figure 3.11. SEM images of 400-Ni mesh (a) before and (b, c, d) after Zn electrodeposition

The overall approach in this part of the thesis was to use electrodeposition to create the Al-Zn particles. A 400-Ni mesh (Figure 3.11 a) was used as the substrate for deposition because of its homogenous grid structure. First, pure Zn was deposited onto the 400-Ni mesh in order to determine if well-controlled Zn particles could be obtained. The Ni mesh working electrode was immersed in 1M $ZnSO_4$ with two Zn rods as counter electrodes, for 30 minutes with a current density of 66.7 mA/cm^2. The SEM images of Ni mesh after Zn deposition are shown in Figure 3.11b-d. It can be clearly seen that after Zn deposition, the

each line of mesh grew bigger and wider and the coating is homogeneous and dense. Although the structure of the Zn was different than the Zn coating on Al wires, the adhesion and crystallinity were both very good.

Next, to co-deposit Al and Zn, an Al precursor needed to be added to the electrodeposition bath. One issue that was encountered when adding Al ions to the deposition bath was Al^{3+} hydrolysis, which led to the formation of white-colored solids as shown in Figure 3.12.

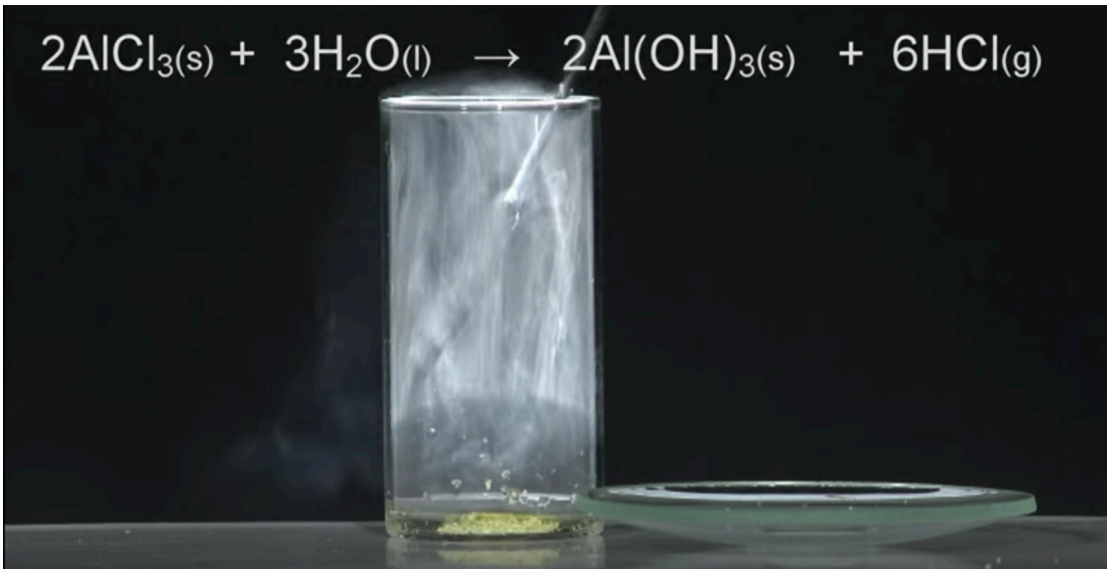

Figure 3.12. Al^{3+} hydrolysis phenomenon for $AlCl_3$

Take aluminum chloride as an example; it is hygroscopic and it fumes in moist air and hisses when mixed with liquid water as the Cl^- ions are displaced with H_2O molecules in the lattice to form the hexahydrate $[Al(H_2O)_6]Cl_3$ (also white to yellowish in color). Then:

$$Al(H_2O)_6Cl_3 \rightarrow Al(OH)_3 + 3HCl + 3H_2O \quad (6)$$

Aluminum chloride is not the only precursor where this issue was observed. For instance, aluminum sulfate also reacts with water by Al^{3+} hydrolysis, as shown in Equation 7.

$$Al_2(SO4)_3 + 6H_2O \rightarrow 2Al(OH)_3 + 3H_2SO_4 \quad (7)$$

(a) (b)

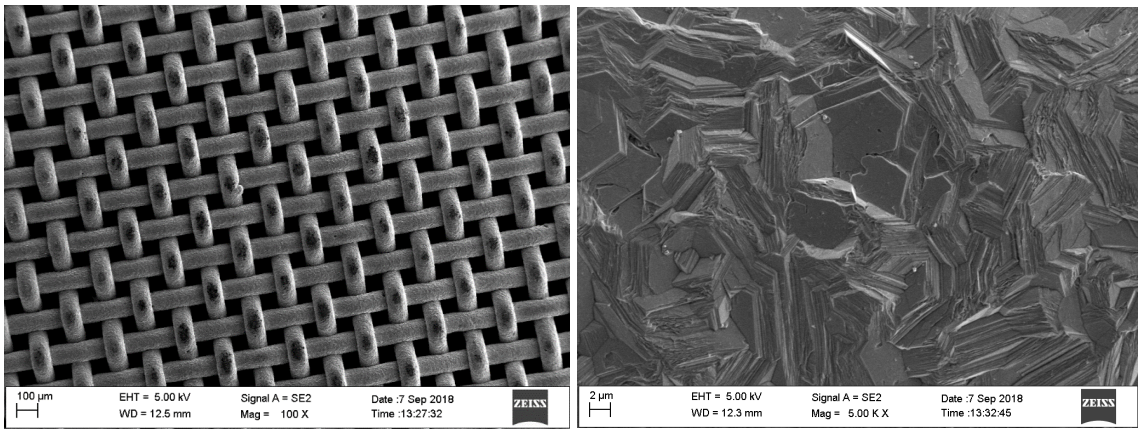

Figure 3.13. (a, b) SEM images of 400-Ni mesh after Al-Zn electrodeposition employing 1M $ZnSO_4$ + 0.01M $AlCl_3$

One safety implication of these reactions is that aluminum salts should be added to solutions under a fume hood. On a practical side, one way to reduce the hydrolysis, and to produce solid-free solutions with both Al and Zn ions in controllable concentrations is to add a small amount of acid to the deposition bath. While $AlCl_3$ was used in this deposition electrolyte, the typical acid and acid concentration used in this study were HCl at 100 ppm. The reason that the addition of acid is effective in curbing hydrolysis is that when $AlCl_3$ was added to water, a reversible reaction takes place, which means it could proceed in both the forward and backward directions, as shown in Equation 8.

$$AlCl_3 + 3H_2O \leftrightarrow Al(OH)_3 + 3HCl \quad (8)$$

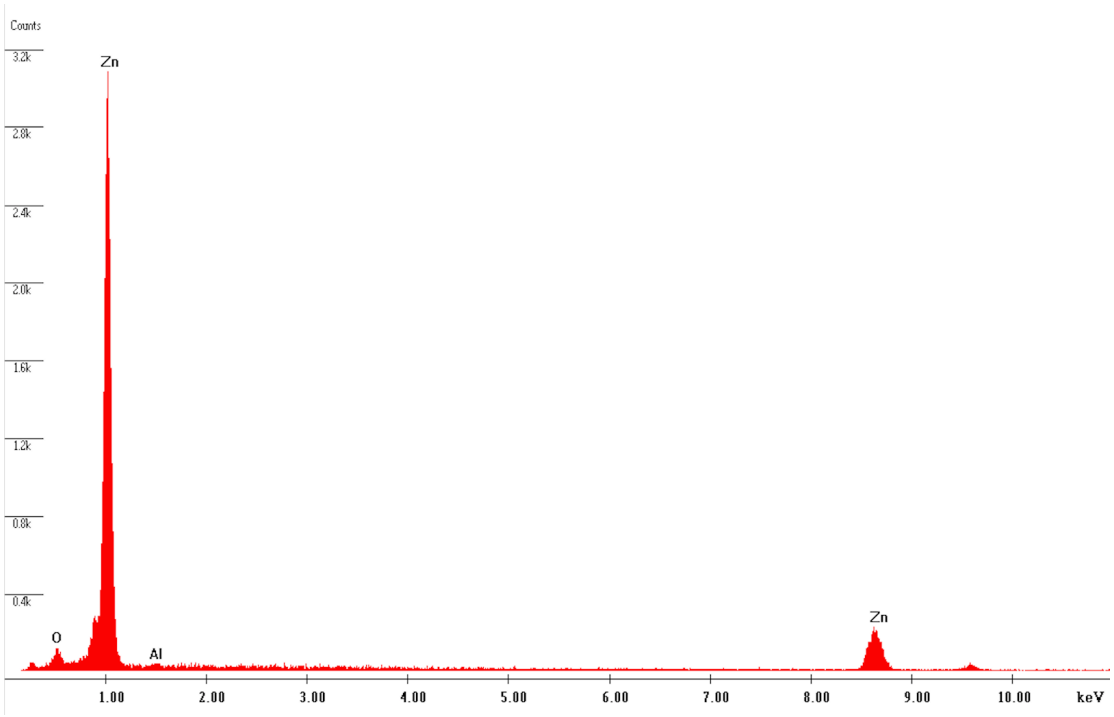

Figure 3.14. EDS results of 400-Ni mesh after Al-Zn electrodeposition employing 1M $ZnSO_4$ + 0.01M $AlCl_3$

Thus, due to "The Equilibrium Law", adding a bit of HCl would shift the equilibrium to the left side to inhibit hydrolysis. Various amounts of $AlCl_3$ were added to the 1M $ZnSO_4$ electrodeposition bath, as is shown in Table 3.3.1. In these experiments, the deposition time was held at 30 minutes with a current density of 66.7 mA/cm^2 at room temperature. As shown in Figure 3.13a-b, SEM images of 400-Ni mesh after Al-Zn electrodeposition employing 1M $ZnSO_4$ + 0.01M $AlCl_3$ indicates that adding $AlCl_3$ to electrolyte would lead to a thinner layer on 400-Ni mesh than the Zn one above. The coating is homogeneous with a little bit of a change in structure as well as tighter adhesion. From the EDS results (Figure 3.14) below, the Al and Zn content were 1.4wt% and 98.6wt%, respectively. Then, the theoretical capacity was calculated based on a

gravimetric weighting, Equation 9, and the calculated values for each of the Al-Zn samples applying various amounts of $AlCl_3$ is provided in Table 3.5.

$$\text{Theoretical } C_{alloy} = X_{Al} * \text{Theoretical } C_{Al} + X_{Zn} * \text{Theoretical } C_{Zn} \quad (9)$$

Next, the achievable capacity for the Al-Zn anode materials was determined by discharging the particle-coated Ni mesh for 3 hours at a current density of 30 mA/cm^2. After discharge, the mass of the electrode was measured and Equation 1 was used to calculate the capacity. The achieved capacity for each of the electrodes is given in the rightmost column of Table 3.5. With higher Al content in the alloy, it was confirmed that a higher capacity could be achieved. This result clearly showed that the Al incorporated into the Zn particles could be electrochemically utilized during discharge.

Table 3.5. Influence of adding Al to electrodeposited Zn on capacity

Al Concentration in 1M $ZnSO_4$ (M)	Al Content (wt %)	Al Content (at %)	Theoretical Capacity (mAh/g)	Achieved Capacity (mAh/g)
0.00	0.00	0.00	820	794 ± 18
0.01	1.33	2.55	850.3	820 ± 14
0.05	1.1	2.4	861.8	846 ± 21

The next step was to evaluate the corrosion rate of the Al-Zn particles. The samples employing various Al concentrations – 0, 0.01 and 0.05M – in 1M $ZnSO_4$ showed H_2 gassing rates of 22.7, 90.7 and 160.2 uL/min/cm^2, respectively, which proves that adding Al increases the corrosion rate due to Al corrosion. Another method to determine the corrosion rate of a surface is linear sweep voltammetry. Linear sweep voltammograms were collected for both of the Al-Zn particles at a scan rate of 0.2 mV/s in 35% KOH electrolyte at room temperature and a Tafel analysis was performed. A typical linear sweep voltammogram is shown in Figure 3.15a. There are two curves including anodic and

cathodic polarization. On the left it shows anodic Tafel region where Zn dissolution takes place, Equation 10:

$$Zn + 4OH^- \rightarrow Zn(OH)_4^{2-} + 2e^- \quad (10)$$

On the right it shows cathodic Tafel region where H_2 evolution and Zn deposition happen, Equation 11-12:

$$2H^+ + 2e^- \rightarrow H_2 \quad (11)$$

$$Zn(OH)_4^{2-} + 2e^- \rightarrow Zn + 4OH^- \quad (12)$$

This corrosion analysis was done in 35% KOH with a) no dissolved ZnO, b) 2 wt% dissolved ZnO, and c) saturated ZnO. As is shown in Figure 3.15 (b, c), these two samples employing varied Al content share the same trend that the corrosion current decreases with the addition of ZnO. This is consistent with commercial alkaline batteries where ZnO is added to commercial cells to reduce Zn corrosion by making it less favorable thermodynamically.

Another note is that the corrosion rates in Figure 3.15b-c are very similar to (actually slightly lower than) the values that were measured for the Al-free Zn particles using the same method. This is promising, because it is already known that Zn has acceptably low rates for corrosion and H_2 gassing during on-the-shelf and non-abuse discharge conditions. This suggests that at least some Al incorporation to increase capacity can be done without sacrificing stability and safety. However, further study will be needed to understand this more fully.

(a)

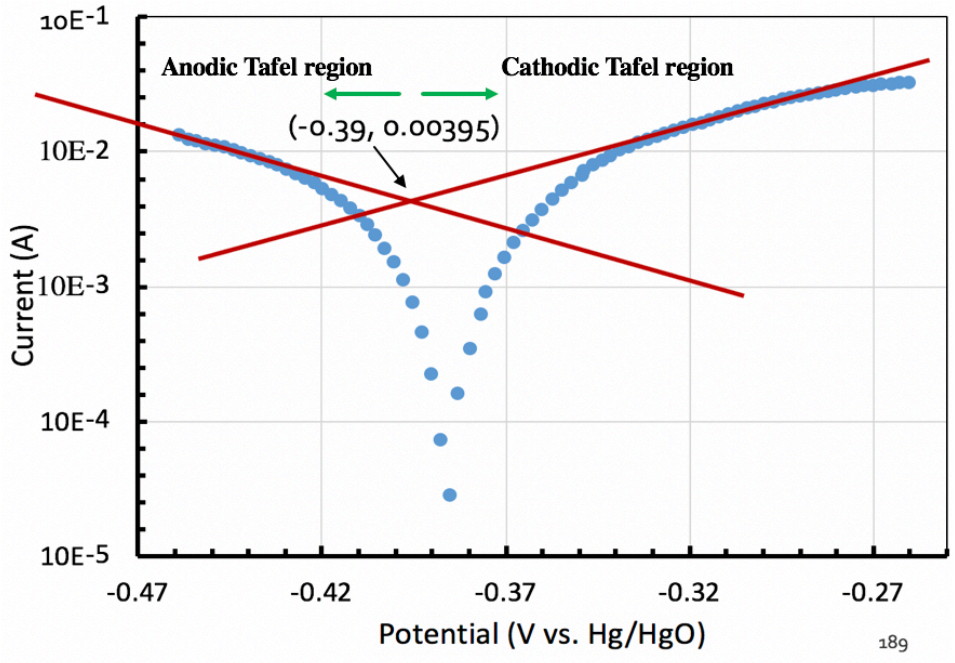

(b) (c)

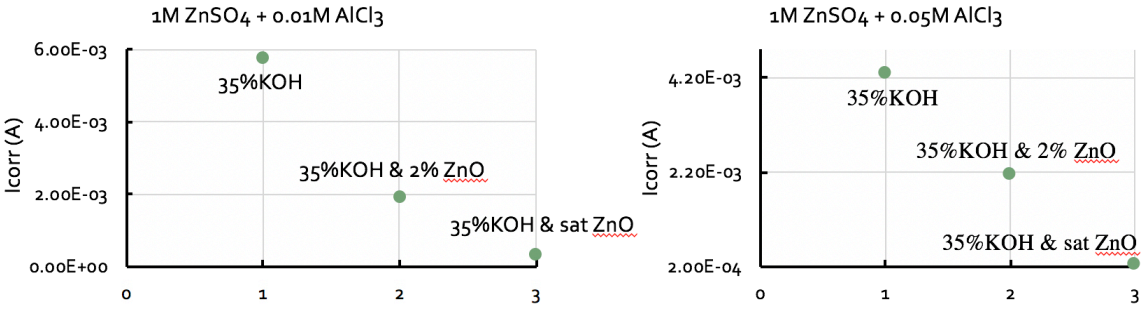

Figure 3.15. (a) i-E polarization curve with the scan rate of 0.2 mV/s in 35% KOH at room temperature and (b, c) corrosion current in different solutions

CHAPTER 4

CONCLUSIONS

In this thesis, the influence of Zn coatings for Al protection in alkaline batteries has been studied. Different methods have been used to deposit Zn films onto Al substrates, with the deepest focus on Zn electrodeposition onto Al wire electrodes under various experimental conditions. Zn was first deposited onto Al wires using a 3-electrode cell. Electrolytic bath additives including Cl^- and PEG400 were introduced into the 1M $ZnSO_4$ solution during electrodeposition. Very small amounts ($\leqslant$ 5 ppm) of Cl^- ions can help to adsorb PEG onto the Al surface. The structure and electrochemical behavior of the resulting Zn-coated Al were characterized. The adhesion and crystallinity of the deposits improved with adding Cl^- ions and PEG and a lower porosity deposit was achieved. All of the films deposited from a 1%PEG + 1M $ZnSO_4$ + ($\leqslant$ 5 ppm) HCl electrolyte showed a 99% reduction in H_2 gassing compared to bare Al wires, and more than twice the capacity of Zn was achieved – though the electrolyte with 2.5 ppm Cl^- did show the highest capacity. It was even shown that this deposition process was repeatable with partial discharges.

After successful demonstration of Zn deposition onto Al wires, the next phase of the project was focus on moving away from wires and examining the creation of Zn-coated Al particles for use in realistic battery systems. 1M $ZnSO_4$ + 1%PEG + 2.5PPM HCl+ 0.3M Sodium hypophosphite bath was explored for electroless deposition to form Zn-coated Al.

The microparticles that were grown were too large to form a thin and efficient layer and due to the inter-particle spacing, the sample had a relatively high H_2 gassing rate. Hence, it has been discovered that electrodeposition was a far more effective method to produce Zn particles than electroless deposition.

Therefore, an alternative approach to utilizing (at least some of) the Al capacity while maintaining a low-corrosion material is to create Zn-rich Al-Zn alloys. With higher Al content in the alloy, it was confirmed that a higher capacity could be achieved. This result clearly showed that the Al incorporated into the Zn particles could be electrochemically utilized during discharge.

REFERENCES

1. Gallaway, J. W.; Menard, M.; Hertzberg, B.; Zhong, Z.; Croft, M.; Sviridov, L. A.; Turney, D. E.; Banerjee, S.; Steingart, D. A.; Erdonmez, C. K., Hetaerolite profiles in alkaline batteries measured by high energy EDXRD. *Journal of The Electrochemical Society* **2015,** *162* (1), A162-A168.
2. Primary alkaline batteries - Google Search.
3. Zaromb, S., The use and behavior of aluminum anodes in alkaline primary batteries. *Journal of The Electrochemical Society* **1962,** *109* (12), 1125-1130.
4. Application of primary alkaline batteries in radio-controlled aircraft model and electric toys - Google Search.
5. Reddy, T. B., Linden's Handbook of Batteries, Fourth Edition. 2002.
6. Cross-sectional view through a Zn-MnO_2 primary alkaline battery - Google Search.
7. Illustration of the working principles of a Zn-MnO2 primary alkaline battery - Google Search.
8. Powers, R. W.; Breiter, M. W., The anodic dissolution and passivation of zinc in concentrated potassium hydroxide solutions. *Journal of The Electrochemical Society* **1969,** *116* (6), 719-729.
9. Abdel-Gaber, A. M.; Khamis, E.; Abo-ElDahab, H.; Adeel, S., Inhibition of aluminium corrosion in alkaline solutions using natural compound. *Materials Chemistry and Physics* **2008,** *109* (2–3), 297-305.
10. Li, Q.; Bjerrum, N. J., Aluminum as anode for energy storage and conversion: a review. *Journal of Power Sources* **2002,** *110* (1), 1-10.
11. Chang, X.; Wang, J.; Shao, H.; Wang, J.; Zeng, X.; Zhang, J.; Cao, C., Corrosion and anodic behaviors of pure aluminum in a novel alkaline electrolyte. *Acta Physico-Chimica Sinica* **2008,** *24* (9), 1620-1624.
12. Emregül, K. C.; Aksüt, A. A., The behavior of aluminum in alkaline media. *Corrosion Science* **2000,** *42* (12), 2051-2067.
13. Mercier, D.; Barthés-Labrousse, M. G., The role of chelating agents on the corrosion mechanisms of aluminium in alkaline aqueous solutions. *Corrosion Science* **2009,** *51* (2), 339-348.
14. Abdel-Gaber, A. M.; Khamis, E.; Abo-Eldahab, H.; Adeel, S., Novel package for inhibition of aluminium corrosion in alkaline solutions. *Materials Chemistry and Physics* **2010,** *124* (1), 773-779.
15. Amin, M. A.; Ei-Rehim, S. S. A.; El-Sherbini, E. E. F.; Hazzazi, O. A.; Abbas, M. N., Polyacrylic acid as a corrosion inhibitor for aluminium in weakly alkaline solutions. Part I: Weight loss, polarization, impedance EFM and EDX studies. *Corrosion Science* **2009,** *51* (3), 658-667.
16. Xhanari, K.; Finšgar, M., Organic corrosion inhibitors for aluminum and its alloys in chloride and alkaline solutions: A review. *Arabian Journal of Chemistry* **2016**.

17. Kavitha, B.; Santhosh, P.; Renukadevi, M.; Kalpana, A.; Shakkthivel, P.; Vasudevan, T., Role of organic additives on zinc plating. *Surface and Coatings Technology* **2006,** *201* (6), 3438-3442.
18. Wang, X. Y.; Wang, J. M.; Shao, H. B.; Zhang, J. Q.; Cao, C. N., Influences of zinc oxide and an organic additive on the electrochemical behavior of pure aluminum in an alkaline solution. *Journal of Applied Electrochemistry* **2005,** *35* (2), 213-216.
19. Mirkova, L.; Maurin, G.; Krastev, I.; Tsvetkova, C., Hydrogen evolution and permeation into steel during zinc electroplating; effect of organic additives. *Journal of Applied Electrochemistry* **2001,** *31* (6), 647-654.
20. Rashvand avei, M.; Jafarian, M.; Moghanni Bavil Olyaei, H.; Gobal, F.; Hosseini, S. M.; Mahjani, M. G., Study of the alloying additives and alkaline zincate solution effects on the commercial aluminum as galvanic anode for use in alkaline batteries. *Materials Chemistry and Physics* **2013,** *143* (1), 133-142.
21. Powers, R.; Breiter, M., The anodic dissolution and passivation of zinc in concentrated potassium hydroxide solutions. *Journal of the Electrochemical Society* **1969,** *116* (6), 719-729.
22. Bhadra, S.; Hsieh, A.; Wang, M.; Hertzberg, B.; Steingart, D., Anode characterization in zinc-manganese dioxide AA alkaline batteries using electrochemical-acoustic time-of-flight analysis. *Journal of The Electrochemical Society* **2016,** *163* (6), A1050-A1056.
23. Hammouda, B., Physical Characterization Methods p44.
24. Paramasivam, M.; Jayachandran, M.; Venkatakrishna Iyer, S., Influence of alloying additives on the performance of commercial grade aluminium as galvanic anode in alkaline zincate solution for use in primary alkaline batteries. *Journal of Applied Electrochemistry* **2003,** *33* (3), 303-309.
25. Ballesteros, J. C.; Díaz-Arista, P.; Meas, Y.; Ortega, R.; Trejo, G., Zinc electrodeposition in the presence of polyethylene glycol 20000. *Electrochimica Acta* **2007,** *52* (11), 3686-3696.
26. Banik, S. J.; Akolkar, R., Suppressing dendrite growth during zinc electrodeposition by PEG-200 additive. *Journal of The Electrochemical Society* **2013,** *160* (11), D519-D523.
27. T. P. Moffat, D. W., and D. Josell, Electrodeposition of Copper in the SPS-PEG-Cl Additive
System Journal of The Electrochemical Society, 2004; pp C262-C271.
28. Ehsan Faegh, ∗ Travis Omasta,; 1, ∗ Matthew Hull, 3 Sean Ferrin, 3 Sujan Shrestha, 1 Jeremy Lechman, 4 Dan Bolintineanu, 4 Michael Zuraw, 3 and William E. Mustain, Understanding the Dynamics of Primary Zn-MnO 2 Alkaline Battery Gassing with Operando Visualization and Pressure Cells Journal of The Electrochemical Society, 2018; pp 165 (11) A2528-A2535
29. Kirill BORDO, H.-G. n. R., Effect of Deposition Rate on Structure and Surface Morphology of Thin
Evaporated Al Films on Dielectrics and Semiconductors MATERIALS SCIENCE: 2011; pp ISSN 1392–1320.
30. Basker Veeraraghavan, H. K., Branko Popov, Optimization of electroless Ni–Zn–P deposition process: experimental study and mathematical modeling. Electrochimica Acta 49, 2004; pp 3143–3154